

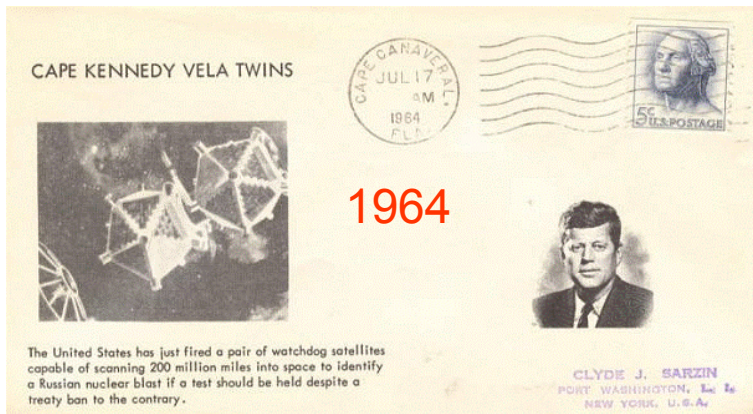
GRBs and CC-SNe: Prospects for LIGO-Virgo/KAGRA searches of long gravitational wave bursts

Maurice H.P.M. van Putten

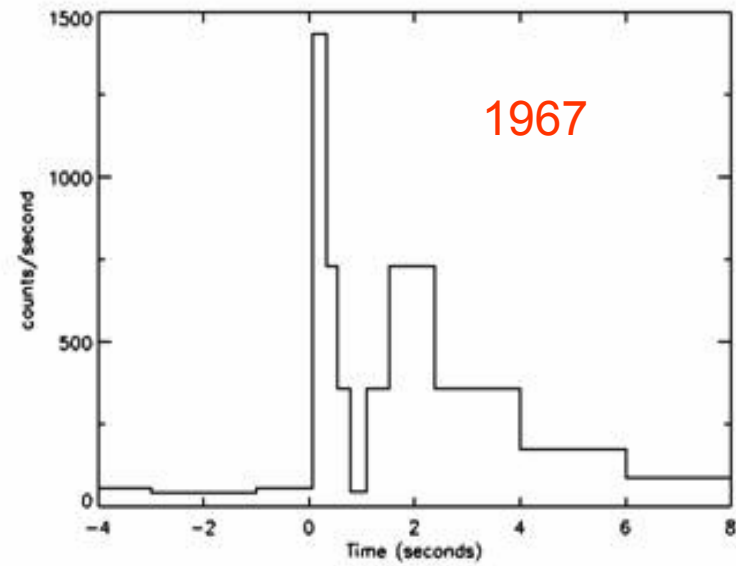
January 2014

Klebesadel, R.W., Strong, I.B., & Olson, R.A., 1973, ApJ, 182, L85

Discovery of mysterious transients



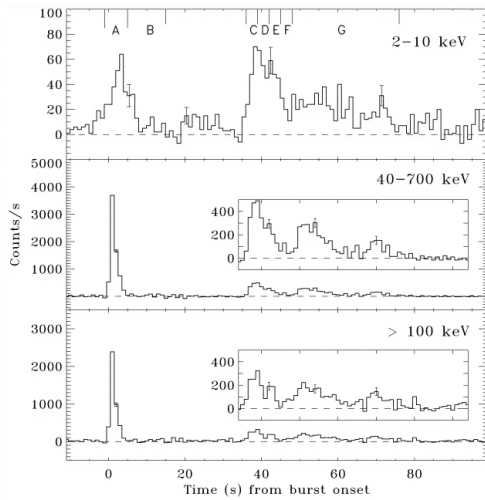
Vela and Konus satellites



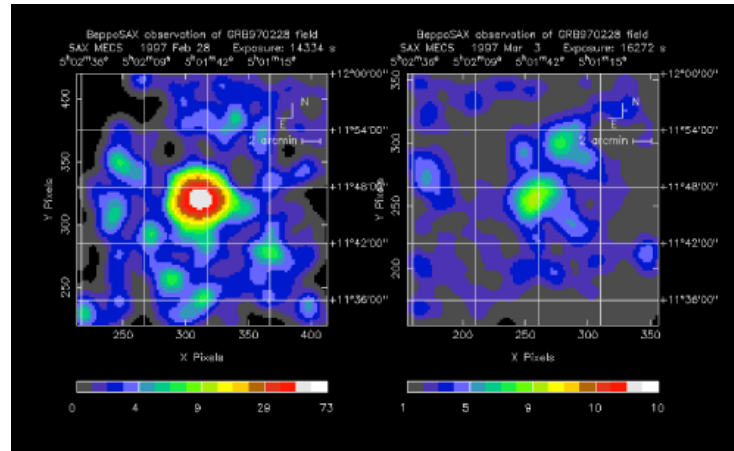


Afterglows

Prompt GRB emission

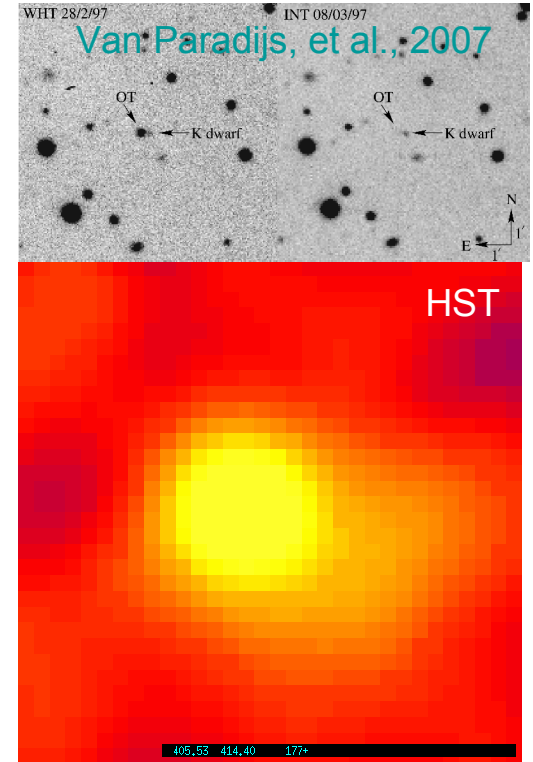


1st X-ray afterglow (+ ~ 8 hr)



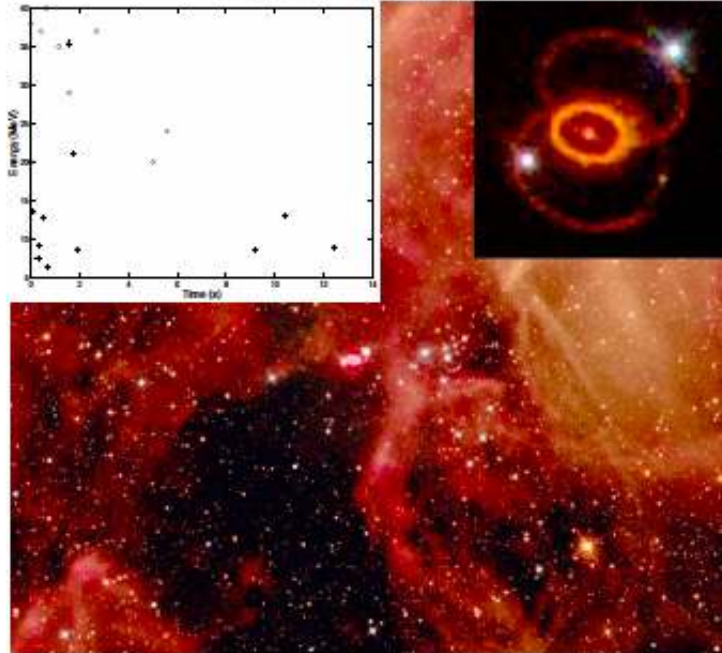
GRB 970228 ($z=0.695$)

Optical Transient



Association with core-collapse SNe

SNI1987A



Radio-loud (Turtle et al. 1987) and aspherical, $> 10 \text{ s} > 10 \text{ MeV}$ neutrino burst, $E_K \sim 1e5 \text{ erg}$ with relativistic jets (Nisenson & Papaliolios 1999) (with BH remnant?)

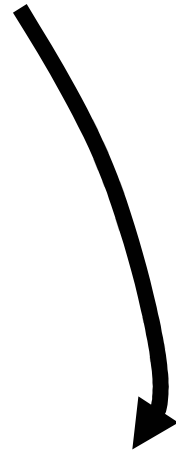
SNI1998bw



Radio-loud and aspherical with $E_K \sim 2e5 \text{ erg}$ ($M_{ej} / 2M_{\odot}$) (Hoeflich et al. 1999) with relativistic ejecta $v_{ej} / c \sim 20\%$ (Wieringa et al. 1999)

Guetta & Della Valle 2007, ApJ, 657, L73; Van Putten, 2004, ApJ, 611, L81

GRB-SNe are rare



Branching ratio of SN Ib/c:

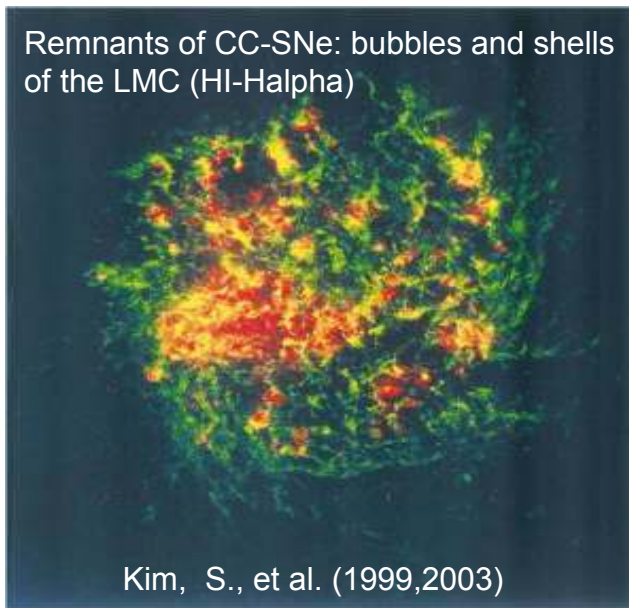
~ 0.2-4 %

Supernova rates:

SN Ia : SN II : SN Ib/c ~ 50:50:10

(depends on survey, e.g., 68:22:7 in PTF)

Remnants of CC-SNe: bubbles and shells of the LMC (HI-Halpha)



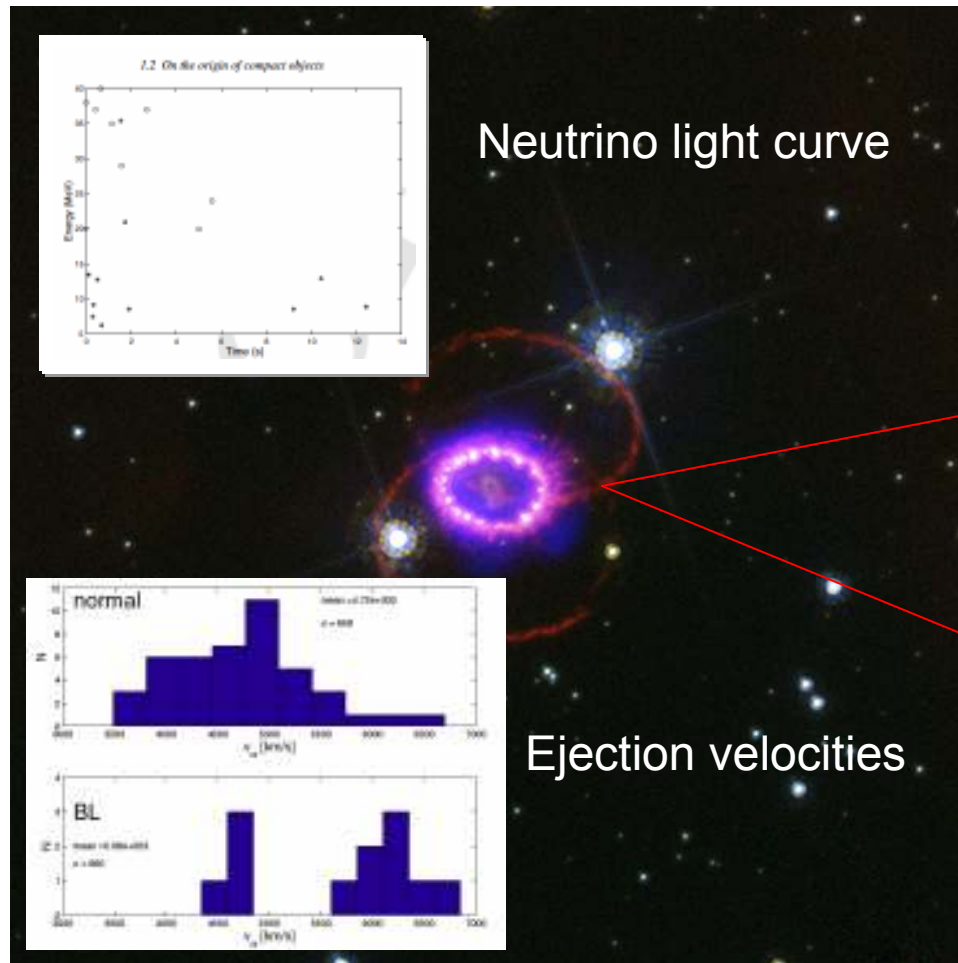
Kim, S., et al. (1999,2003)

(c)2014 van Putten - Ferrara

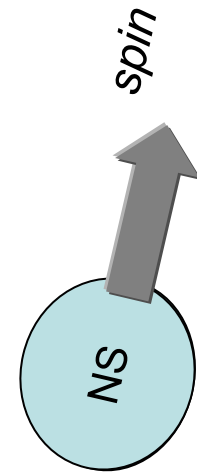
Endpoint of massive stars

Maurer et al. 2010, MNRAS, 402, 161;
Van Putten, Della Valle & Levinson,
2011, A&A, 536, L6

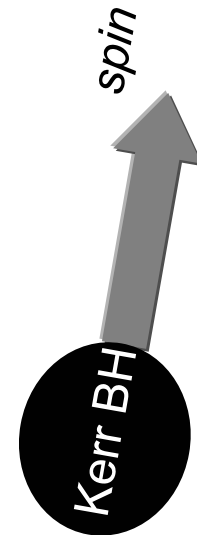
Diversity in NS and BH remnants



3×10^{52} erg (maximal spin, $1.5M_{Sun}$)
 $1\%Mc^2$

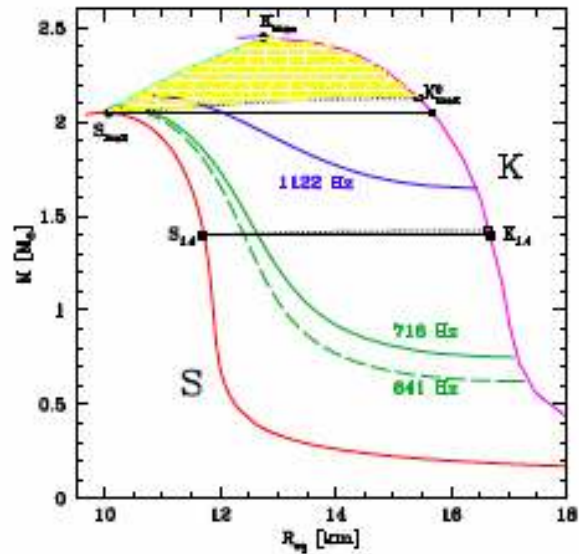


6×10^{54} erg (maximal spin, $10M_{Sun}$)
 $30\%Mc^2$

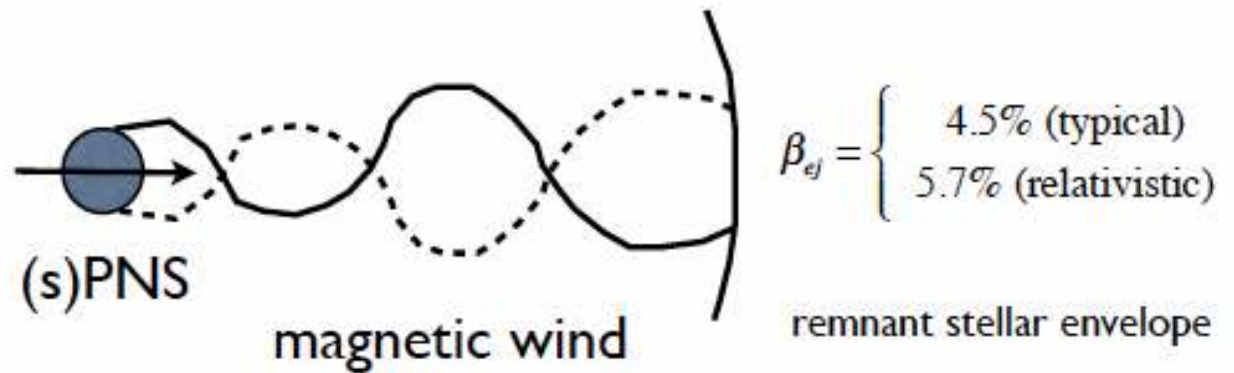


Bisnovatii-Kogan, 1970, Astron. Zh., 47, 813
 Van Putten, Della Valle & Levinson, 2011, A&A, 535, L6

Supernovae from spindown



Haensel et al., 2009, A&A, 502, 605



Efficiency in expelling stellar envelope by magnetic winds:

$$\frac{1}{2}\beta_{ej} < \eta < 1$$

(baryon-poor to baryon-rich winds)

$$E_w = \eta^{-1} E_{SN} \leq E_c$$

$$E_c = \begin{cases} 3 \times 10^{52} \text{ erg (PNS)} \\ 7.5 \times 10^{52} \text{ erg (sPNS)} \\ \text{(supramassive PNS)} \end{cases}$$

Beyond the energy envelope of NS

$$\frac{E_{rot} [\text{required}]}{E_c}$$

Table 1. References refer to SNe except for GRB 070125.

GRB	Supernova	Redshift z	E_γ	E_{tot}	E_{SN}	η	E_{rot}/E_c	Prior	Ref.
	SN2005ap	0.283			>10	1	>0.3	indet	1
	SN2007bi	0.1279			>10	1	>0.3	indet	1
GRB 980425	Sn1998bw	0.008	<0.001		50	1	1.7	BH	2
GRB 031203	SN2003lw	0.1055	<0.17		60	0.25	10	BH	3
GRB 060218	SN2006aj	0.033	<0.04		2	0.25	0.25	indet	4
GRB 100316D	SN2006aj	0.0591	0.037–0.06		10	0.25	1.3	BH	5
GRB 030329	SN2003dh	0.1685	0.07–0.46		40	0.25	5.3	BH	6
GRB 050820A		2.607		42			1.4	BH	7
GRB 050904		6.295		12.9			0.43	indet	7
GRB 070125		1.55		25.3			0.84	indet	7
GRB 080319B		0.937		30			1.0	BH	7
GRB 080916C		4.25		10.2			0.34	indet	7
GRB 090926A		2.1062		14.5			0.48	indet	8
GRB 070125	(halo event)	1.55		25.3			0.84	indet	9

Notes. Energies are in units of 10^{51} erg.

"Orphan" long GRBs

"Long GRBs with no association to massive stars"

TABLE I. Proposed core-collapse and merger progenitors to a Swift sample of long GRBs.

GRB	Redshift	Duration(s)	Host	Constraint ^a	Type
050820A [37,38]	1.71	13 ± 2	UVOT < 1 arcsec	ISM-like [17]	Merger
050904 [39–41]	6.29	225 ± 10	Unseen low star-forming region	Dense molecular cloud [57]	CC-SN
050911	0.165	16	Cluster Edinburgh-Durham Galaxy Catalogue 493	No x-ray afterglow [42]	Merger [58,16]
060418 [43–46]	1.490	(52 ± 1)	ISM spectrum	γ-ray efficiency [17]	Merger
060505 [47]	0.09	4	Spiral, ionized atomic hydrogen	No SN ^b	Merger
060614 [47,50] ^{b,c}	0.13	102	Faint star-forming region	No SN ^{b,c}	Merger [14,15]
070125 [51–53]	1.55	>200	Halo	ISM-like [53]	Merger
080319B [54–56]	0.937	50	Faint dwarf galaxy	Wind [17]	CC-SN

^a"ISM-like" refers to a constant host density; wind refers to a r^{-2} density profile associated with a massive progenitor [35,36].

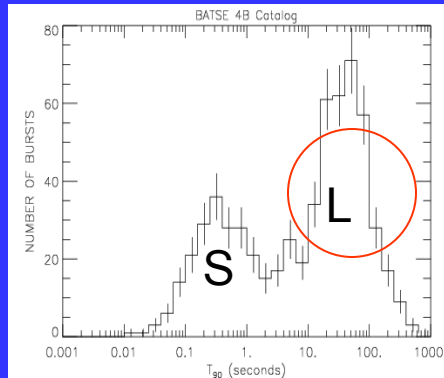
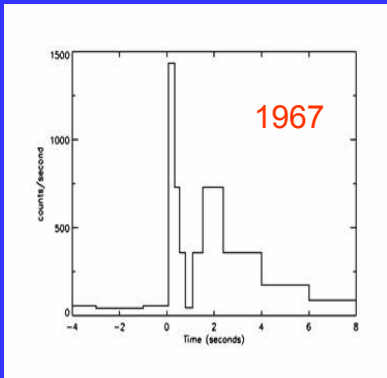
^bObserved with an 8.2 m telescope, [48].

^cObserved with a 1.5 m telescope, [49].

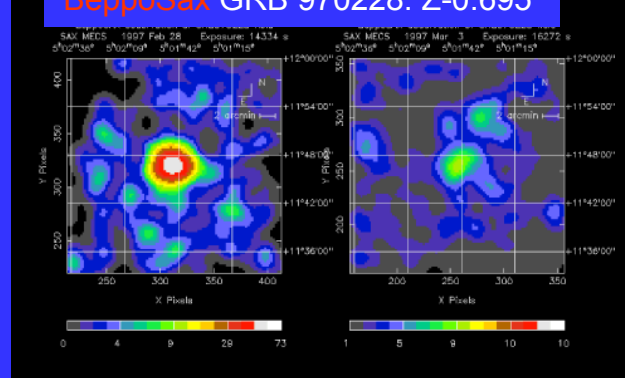
GRB 070125

GRB 060614

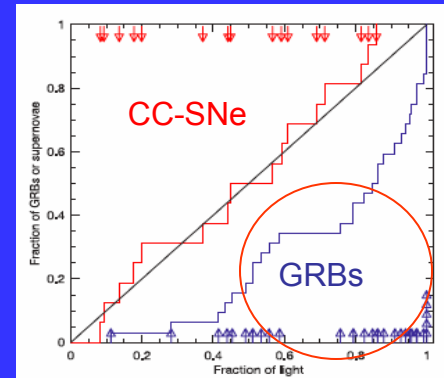
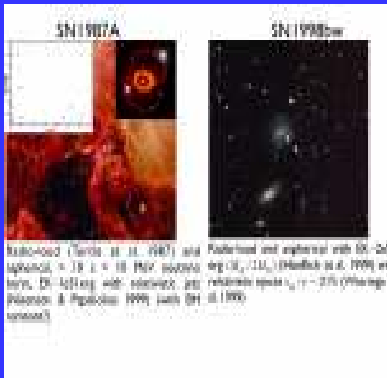
Thumbnail overview...



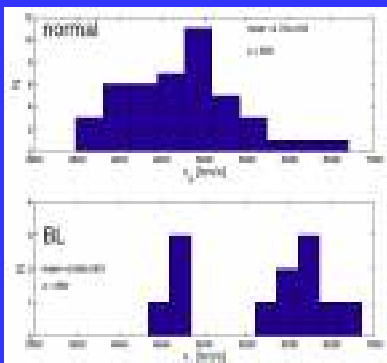
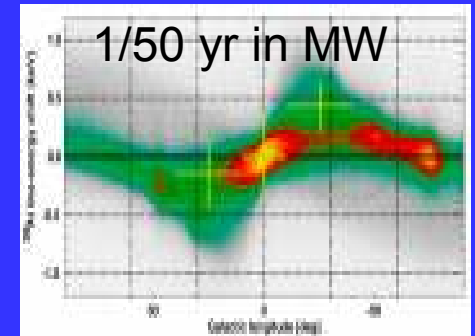
BeppoSax GRB 970228: Z=0.695



Swift, HETE II: X-ray afterglows also to short GRBs 050509B, 050709,...



GRB-SNe are rare making up < 1% of all SN Ib/c and < 0.2% of all CC-SNe



CC-SNe are diverse, NS or BH powered?

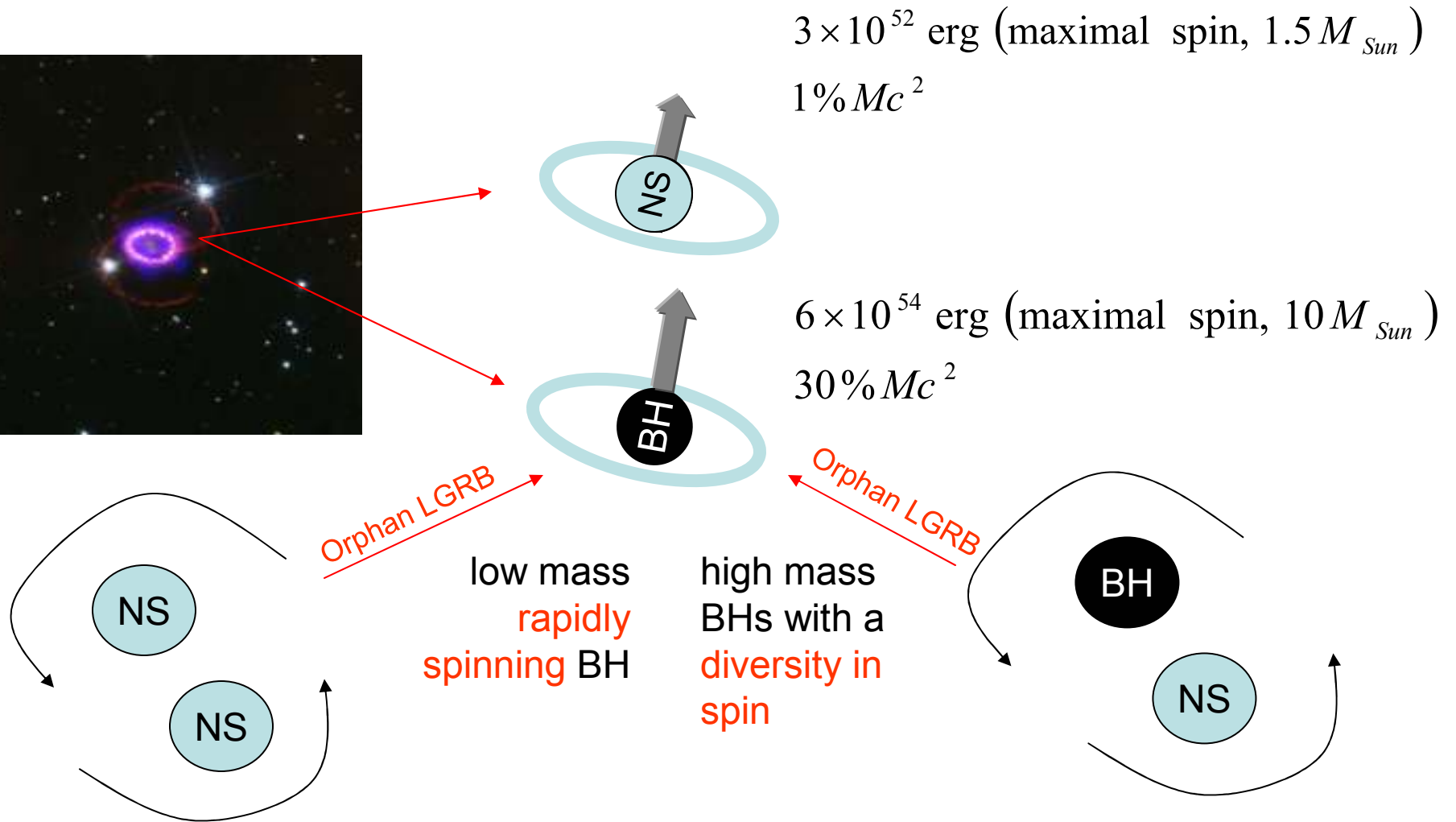
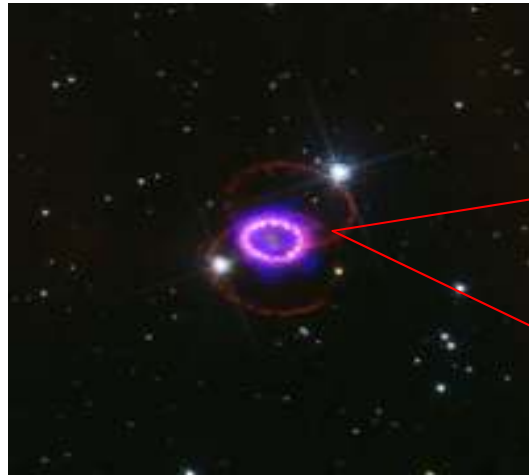
Hyper energetic events (GRB 031203/SN2003lw, GRB030329/SN2003dh defy max Erot of NS)

"Orphan LGRBs" (SGRB-EE) (GRB 059820A, 050911, 060418, 060505, 060614, 070125)

Outline

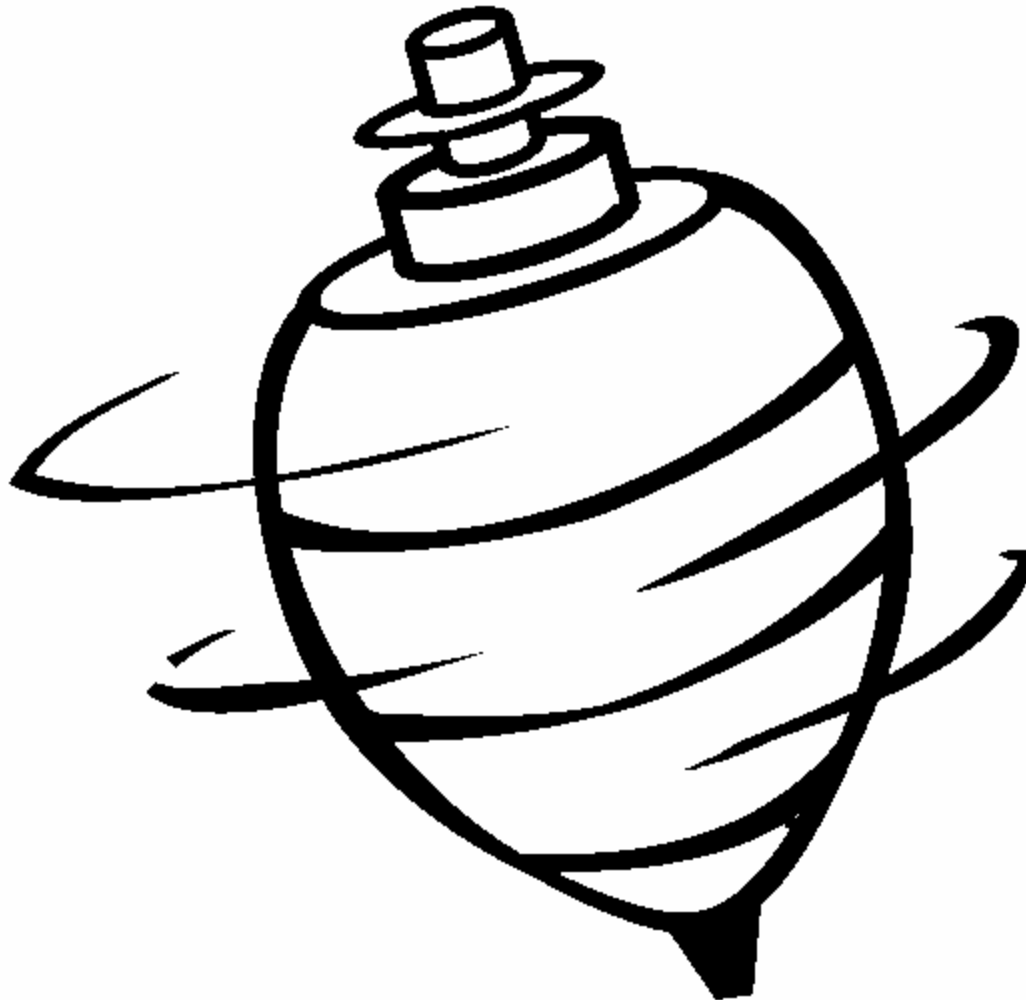
- 1. GRBs from rotating black holes**
2. Probing spindown in the BATSE catalogue of LGRBs
3. Advanced gravitational wave detectors
4. Outlook on broadband GW emission from CC-SNe

Diversity in progenitors



Exact solution to GR
by Roy P. Kerr (1963)

Rotation black hole



www.THECOLOR.com



Rotation black hole ~ spinning top

$$\Omega_H = \frac{1}{2M} \tan(\lambda / 2) \quad \left(\sin \lambda = J / M^2 \right)$$

van Putten, 1999, Science, 284, 115

Maximal spin frequency: 10 kHz for a 10 solar mass black hole

Rotational energy $\left(\frac{E_{rot}}{M} \right)_{BH} = 2 \sin^2(\lambda / 4)$

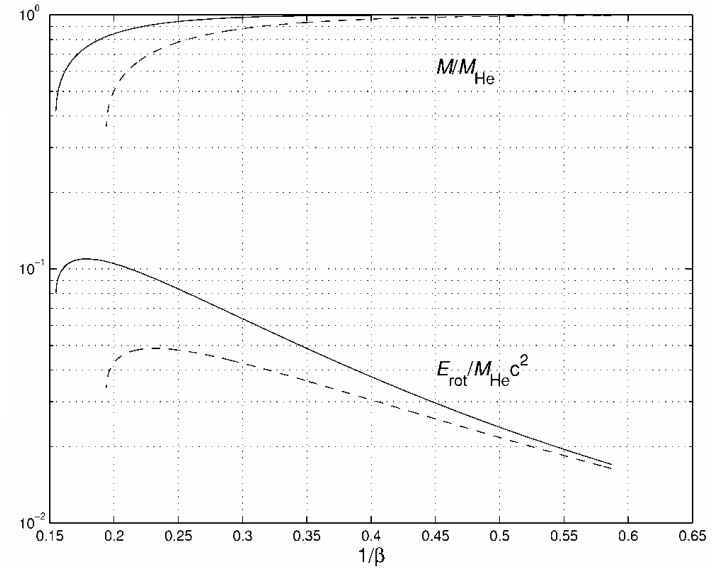
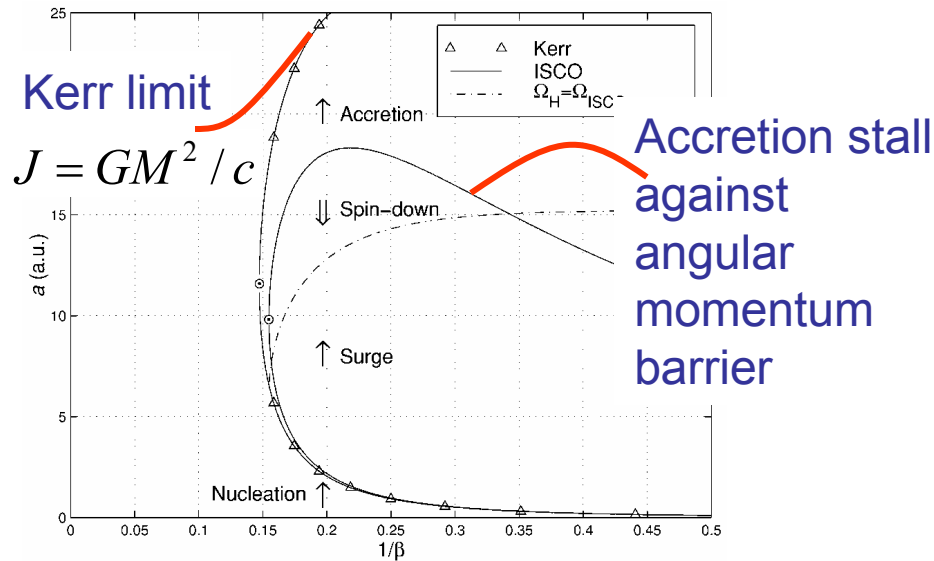
$$\max \left(\frac{E_{rot}}{M} \right)_{BH} = 0.2929 \sim 30 \max \left(\frac{E_{rot}}{M} \right)_{NS}$$

Like a spinning top $\left(\frac{E_{rot}}{\Omega_H J} \right)_{BH} / \left(\frac{E_{rot}}{\omega J} \right)_{Newton(toy)} = 1 - 1.16$

Ib/c SNe in binaries: Woosley, S. E. 1993, ApJ, 405, 273; Paczyn'ski, B. 1998, ApJ, 494, L45

BH formation: Bethe, H. A., Brown, G. E., & Lee, C.-H. 2003, Selected Papers: Formation and Evolution of Black Holes in the Galaxy; Brown, G. E., Lee, C.-H., Wijers R. A. M. J., Lee, H. K., Israelian, G., & Bethe, H. A. 2000, NewA, 5, 191; Van Putten, 2004, ApJ, 611, L81

Making rotating BHs in CC-SNe



$$\beta = 4.22 k_2 P_d^{-1} \left(\frac{M_{He}}{10 M_{Sun}} \right)^{-1/3} \left(k_2 = \frac{2}{3}, 1 \right)$$

Conservative core-collapse in the approximation of spherical or cylindrical geometry

$$P_c = P(v_{kick} < v^*) \cong 0.5\% \left(\frac{v^*}{10 \text{ km s}^{-1}} \right)^2 \left(\frac{\sigma_{kick}}{100 \text{ km s}^{-1}} \right)^{-2}$$

$$E_{rot} \cong (0.3220 - 0.6624) E_{rot}^{\max}$$

With small probability, CC-SNe of envelope stripped stars with intraday binary periods are factories of high mass rapidly rotating BHs

Making rotating BHs in NS-NS mergers

Coalescence NS-NS \rightarrow PNS in merger \rightarrow conservative collapse

$$M_{PNS} \cong 3M_{Sun}, R \cong 14\text{km} :$$

$$E_{rot} \cong 2M \sin^2 \left(\frac{1}{4} \arcsin \left[\frac{2}{5} \sqrt{\frac{R}{R_g}} \Big|_{PNS} \right] \right) \cong 0.4M_{Sun} c^2$$

NS-NS mergers are possibly factories of low mass rapidly rotating BHs

Ampere-like induction

$\mathbf{J} \rightarrow$ rotation of surrounding spacetime rel. distant stars (Mach)

$$ds^2 \cong \text{Schwarzschild + frame dragging} = ds_{Schw}^2 + 2\omega d\varphi dt$$

$$ds_{Schw}^2 = -\alpha^2 dt^2 + \alpha^{-2} dr^2 + r^2 d\vartheta^2 + r^2 \sin^2 \vartheta d\varphi^2$$

$$\alpha = \sqrt{1 - \frac{2M}{r}} = \text{redshift factor}$$

$$\omega = \frac{2J}{\sigma^3}, \quad \sigma^3 = \frac{(r^2 + a^2)^2 - a^2 \Delta \sin^2 \vartheta}{r} \approx \frac{1}{r^3}$$

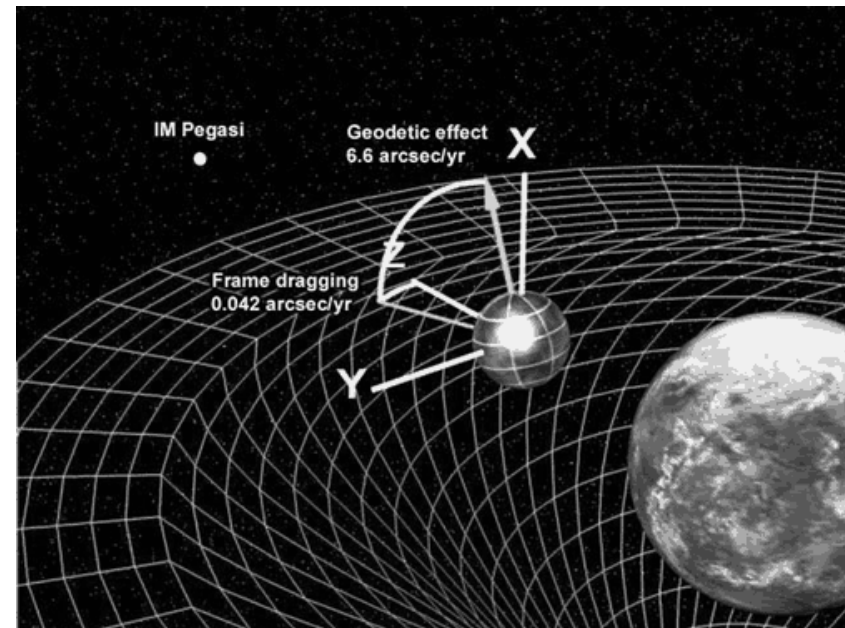
$$ds_{Schw}^2 \cong \text{geodetic precession (GP), perihelion precession (PP)}$$

$$\omega d\varphi dt \cong \text{frame dragging precession}$$

Recent detection of frame dragging

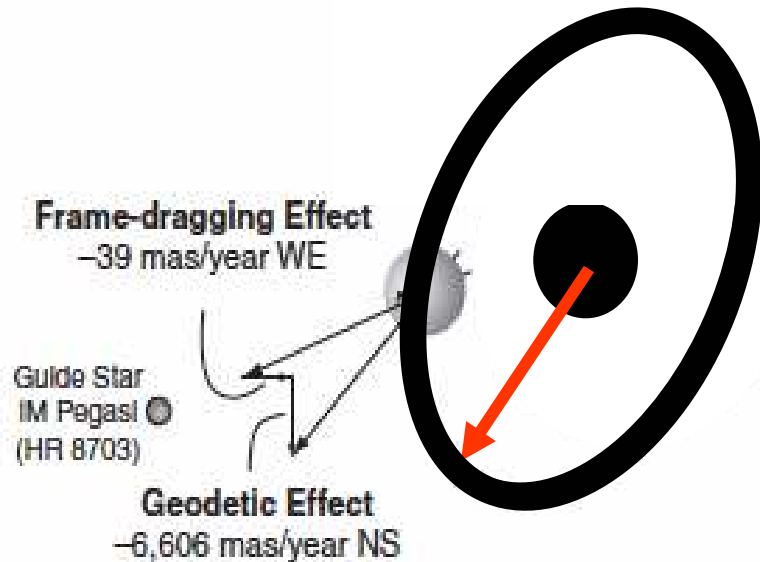
GP-B (orbiting at 642 km):

$$\omega = -39 \text{ marcs/yr}$$



Two complementary experiments:

Everitt, F., et al., 2011, PRL, 106, 221101, Ciufolli, I. & Pavlis, E.C., 2004, Nature, 431, 958

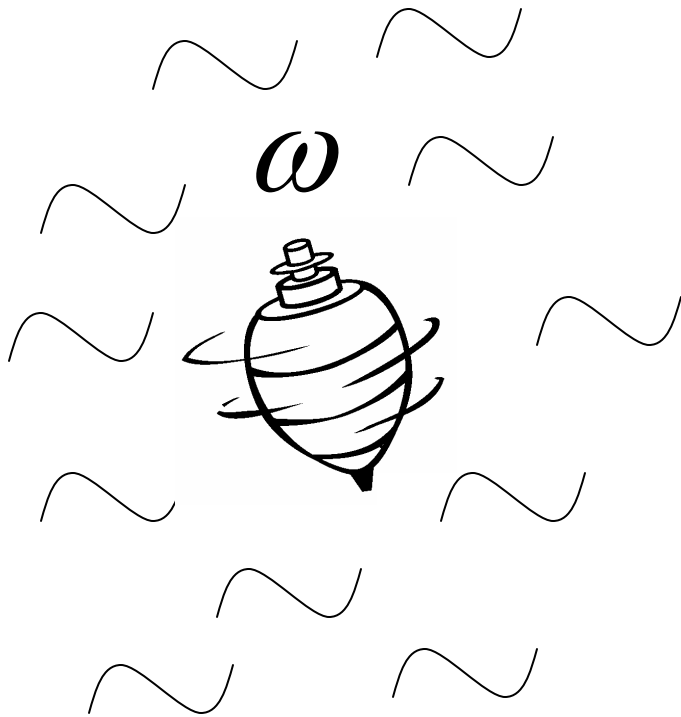


$$\omega \cong \frac{2J}{r^3}$$

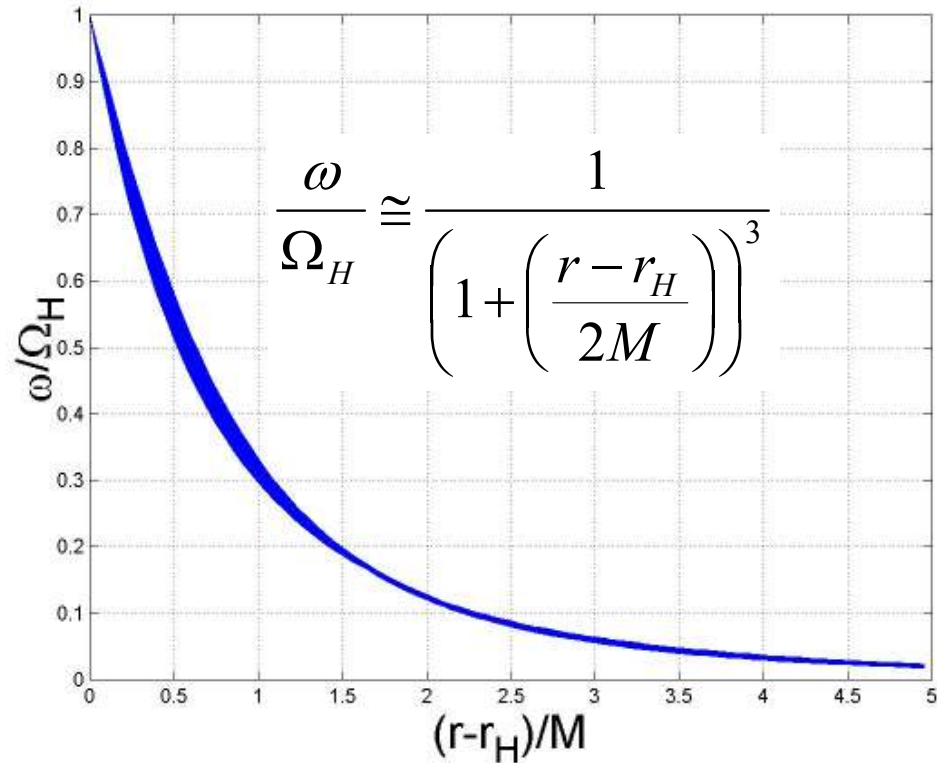
$$r \cong 5 \times 10^6 R_g$$

$$J = M^2 : J = J_{Earth}, M \cong 29 \times M_{Earth}$$

Relativistic frame dragging



$$\omega|_H \equiv \Omega_H$$



Variations with spin: 7.25%

Variations with poloidal angle: 1.67%

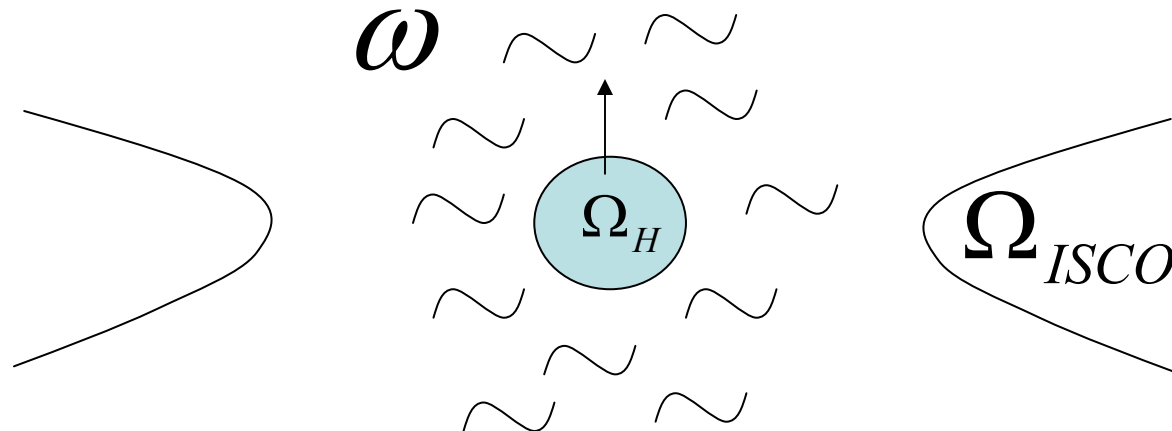
Slow and fast – relative to nearby matter

$$SLOW : \frac{\Omega_H}{\Omega_{ISCO}} < 1 : \frac{E_{rot}}{E_{rot}^{max}} < 6\%$$

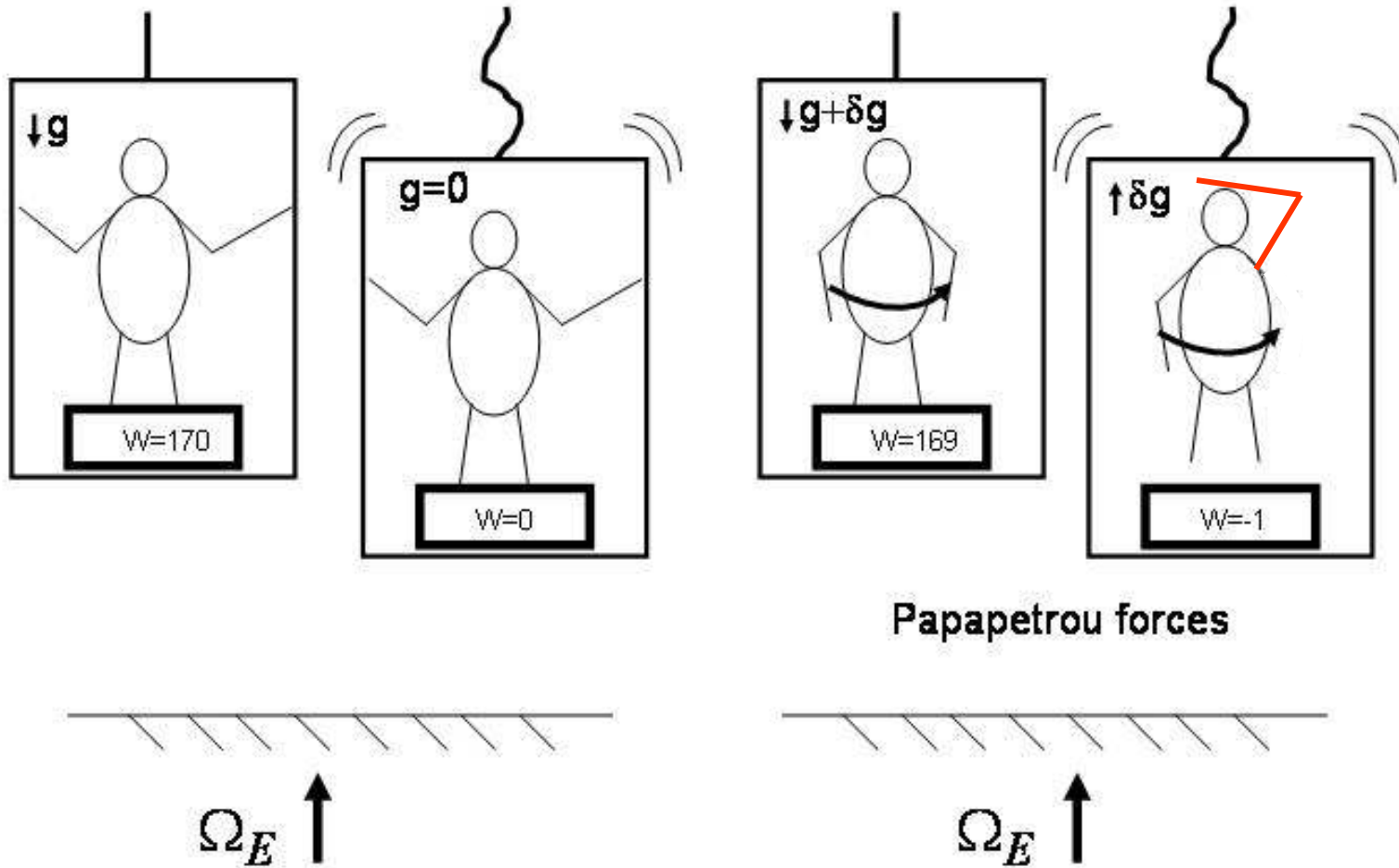
T-magnetically aided
hyperaccretion $\sim T_{90}$ [SGRB]

$$FAST : \frac{\Omega_H}{\Omega_{ISCO}} > 1 : \frac{E_{rot}}{E_{rot}^{max}} > 6\%$$

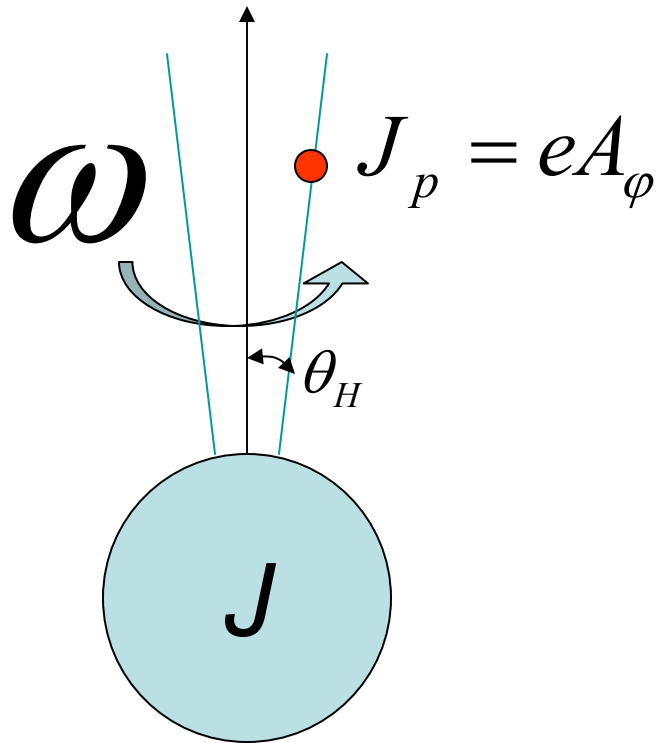
T-spindown $\sim T_{90}$ [LGRB]



ω forces...



ω energies...

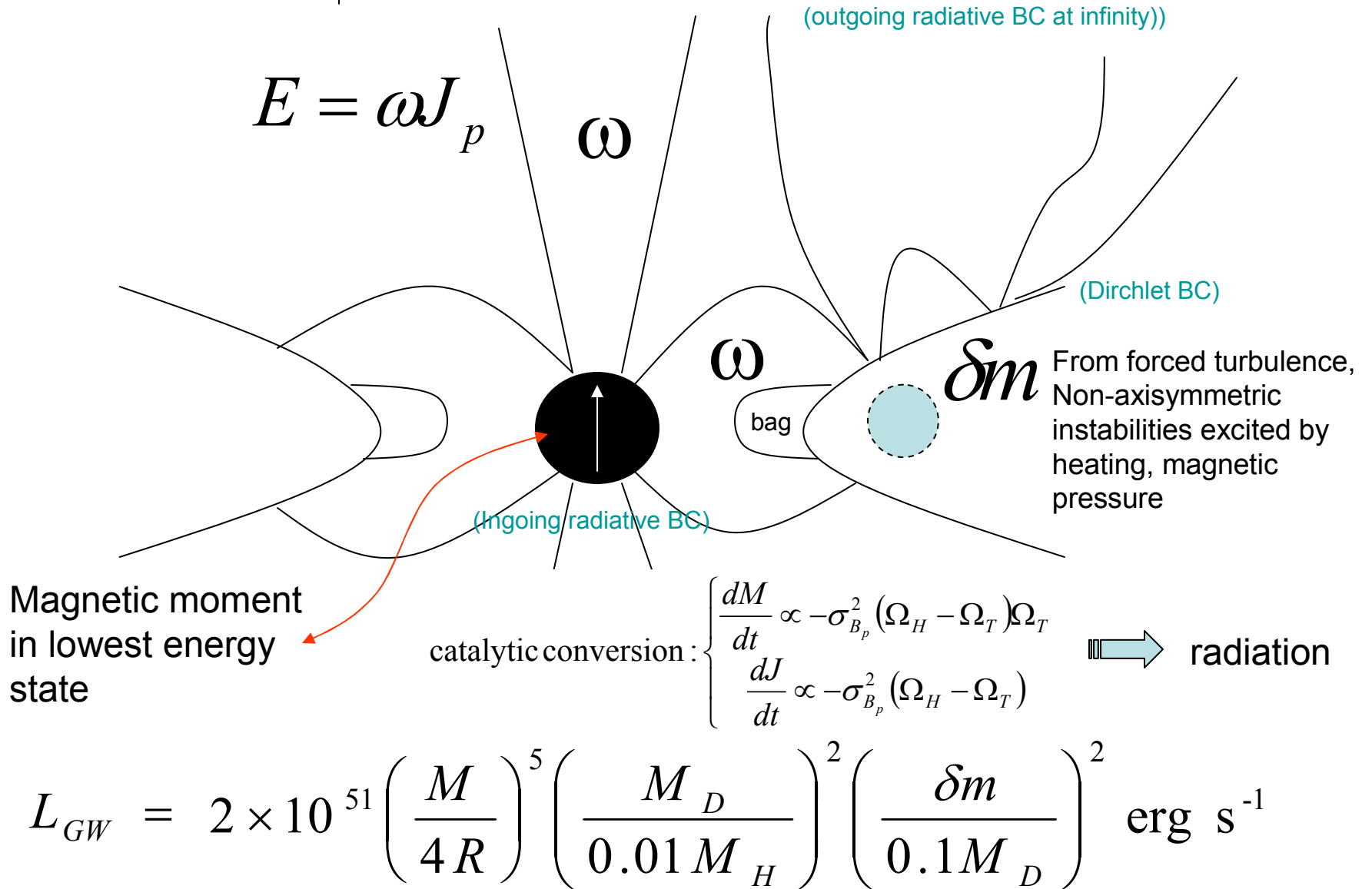


Exact geometric result

$$E = \omega J_p$$

van Putten, 1999, Science, 284, 115; van Putten, 2001, Phys. Rev. Lett., 84, 091101; van Putten & Levinson, 2002, Science, 295, 1874; van Putten, 2002, ApJ, 575, L71; Bromberg, Levinson, van Putten, 2006, NewA, 11, 619; van Putten, 2012, Prog. Theor. Phys., 127,331; van Putten, 2008, ApJ, 684, L91

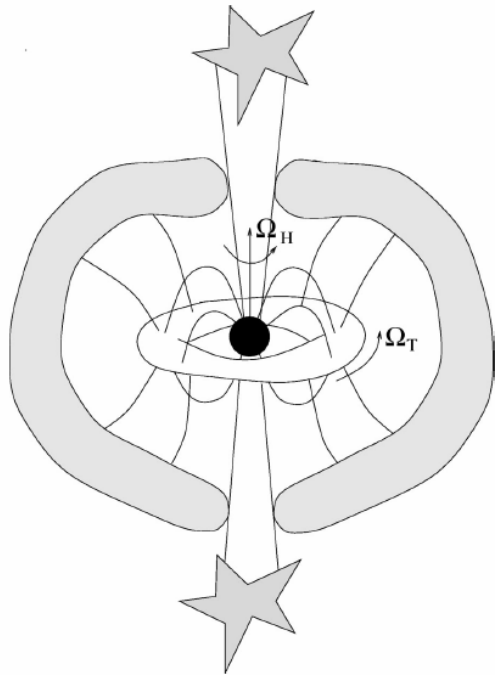
ω radiation processes (non-thermal)



Bisnovatyi-Kogan, 1970, Astron. Zh., 47, 813
 Van Putten, Della Valle & Levinson, 2011, A&A, 536, L6
 Van Putten & Gupta, 2009, MNRAS, 394, 2238
 Van Putten & Levinson, 2003, ApJ, 584, 937
 Van Putten, 2003, 583, 374

T_{90} duration \sim lifetime inner engine \sim lifetime of BH spin

Aspherical explosion



$$\frac{T_{90}}{20 \text{ s}} \cong \left(\frac{0.1 M_{Sun}}{M_D} \right) \left(\frac{M}{7 M_{Sun}} \right)^2 \left(\frac{R_D}{6 R_g} \right)^4$$

$M_D/M \sim \text{const.}$

$\rightarrow E_{kl}[\text{SN}]$ correlated to E_γ

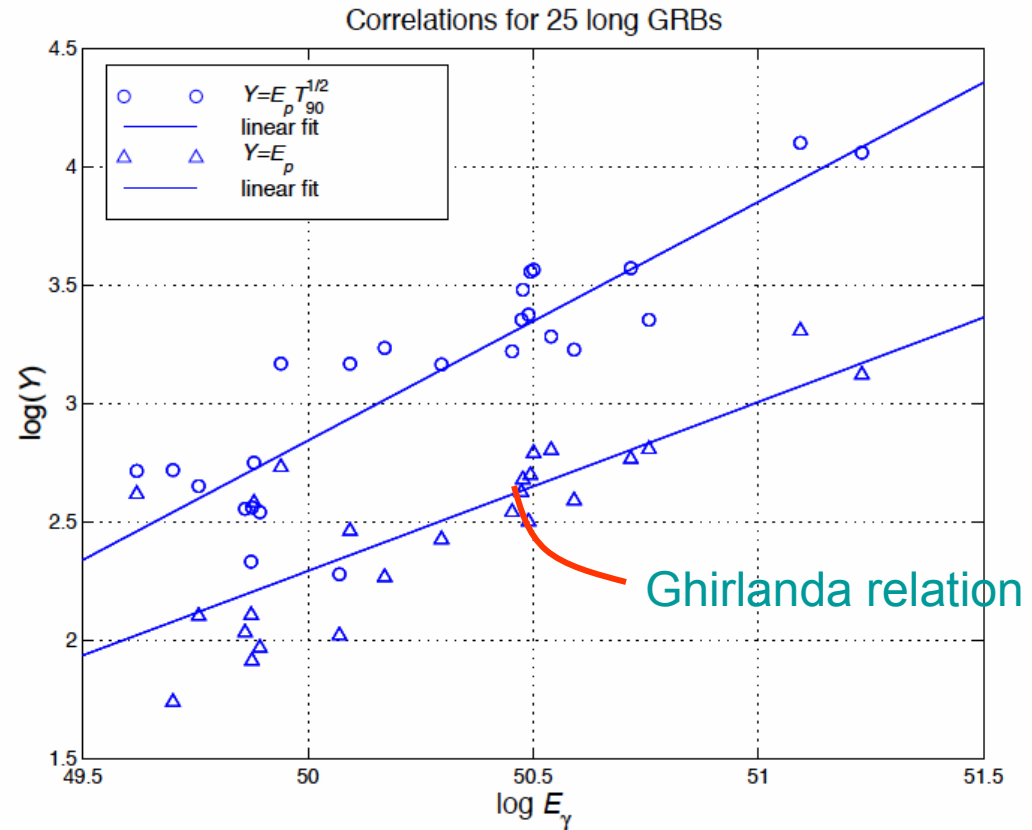
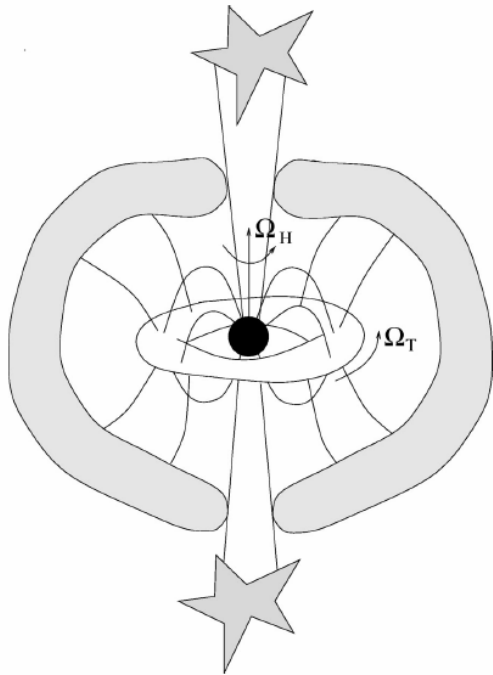
Extends to hr: $M_D < 0.01 M_{Sun}$, $M > 30 M_{Solar}$ ($M_{prog} > 100 M_{Solar}$)

van Putten & Levinson, 2003,
ApJ, 584, 937; van Putten, 2008,
ApJ, 685, L63

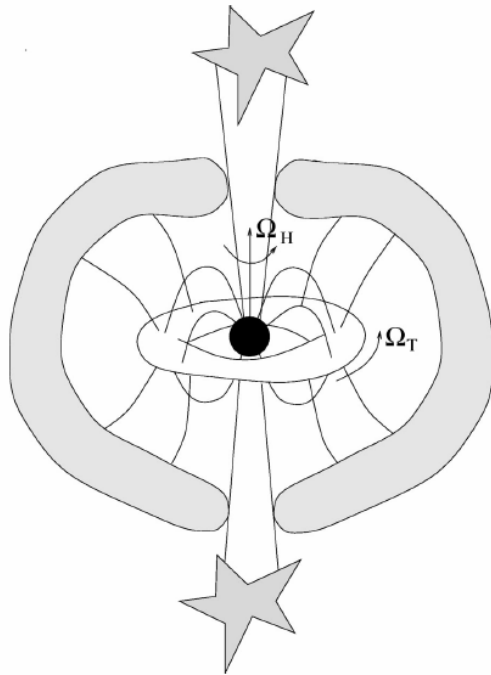
Energy correlation (HETE-II & Swift)

$E = \omega J_p \rightarrow$ Baryon-poor jet $L_H \propto \theta_H^4$

with $E_p T_{90}^{1/2} \propto E_\gamma$



BH vs NS inner engines



Spindown of rotating BH-torus system

SN from baryon rich torus wind,

GRB from baryon-poor jet.

Large reservoir: $E_{rot}[\text{BH}]$

→ Successful GRB and SN

Spindown of a (proto-)NS:

SN, GRB from one magnetic wind
(one baryon loading).

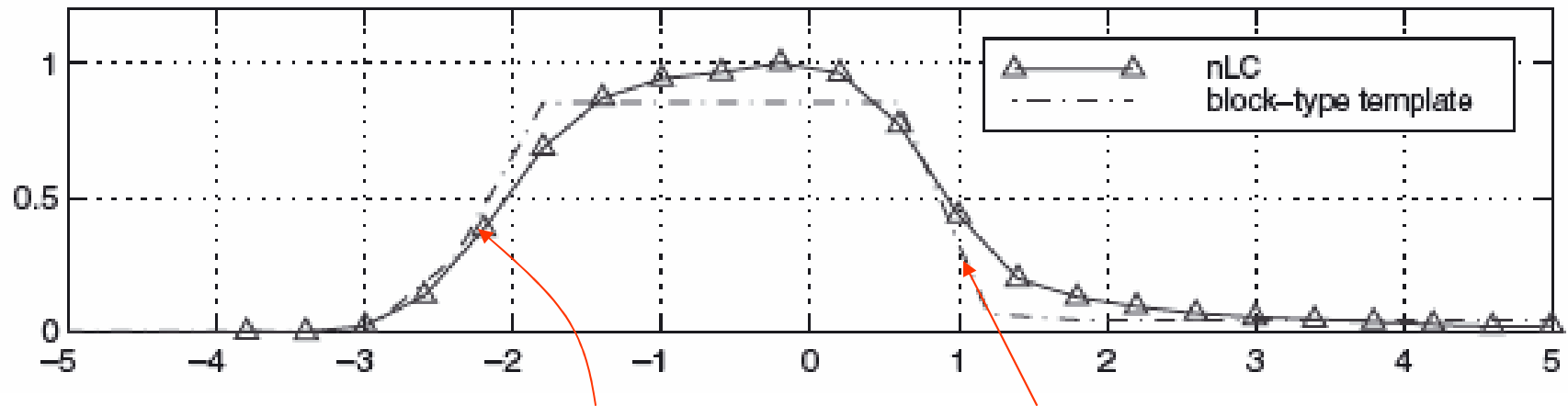
Moderate reservoir: $E_{rot}[\text{NS}]$

→ Either successful GRB or SN

Outline

1. GRBs from rotating black holes
- 2. Probing spindown in the BATSE catalogue of LGRBs**
3. Advanced gravitational wave detectors
4. Outlook on broadband GW emission from CC-SNe

Normalized light curve of long GRBs



normalized light curve

A choice of model light curve

(nLC depends only weakly on choice of template)

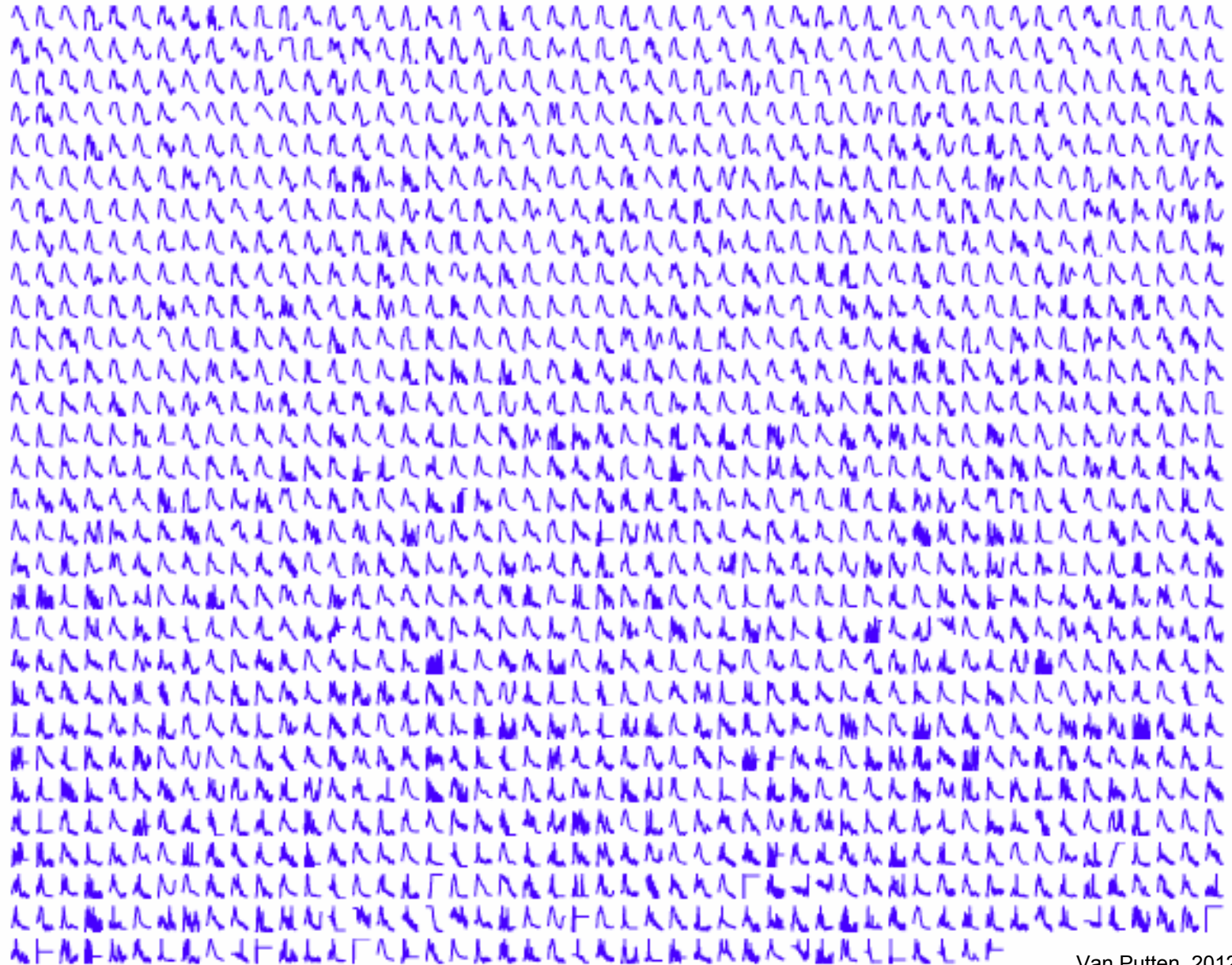


4 parameter matched filtering: scaling in count rate and time with arbitrary shifts (subtraction base line count and offset in time)

Apply to the complete BATSE catalogue of 1491 long GRBs...

BATSE Catalogue of 1491 long GRBs

(smoothed, scaled and ordered by T_{90})



Spindown models

Suspended accretion:

Input from BH balanced with output in GWs, MeV neutrinos and magnetic winds from a torus

$$\tau_+ = \tau_- + \tau_{GW} + \tau_\nu, \quad \Omega_+ \tau_+ = \Omega_- \tau_- + \Omega_T \tau_{GW} + P_\nu,$$

A: $\Omega_T = \Omega_{ISCO}$ matter at ISCO with GW emissions

B: $\Omega_T = \frac{1}{2}\Omega_H$ matter further out with no GW emissions

C: spindown of PNS

nLCs of long GRBs in BATSE

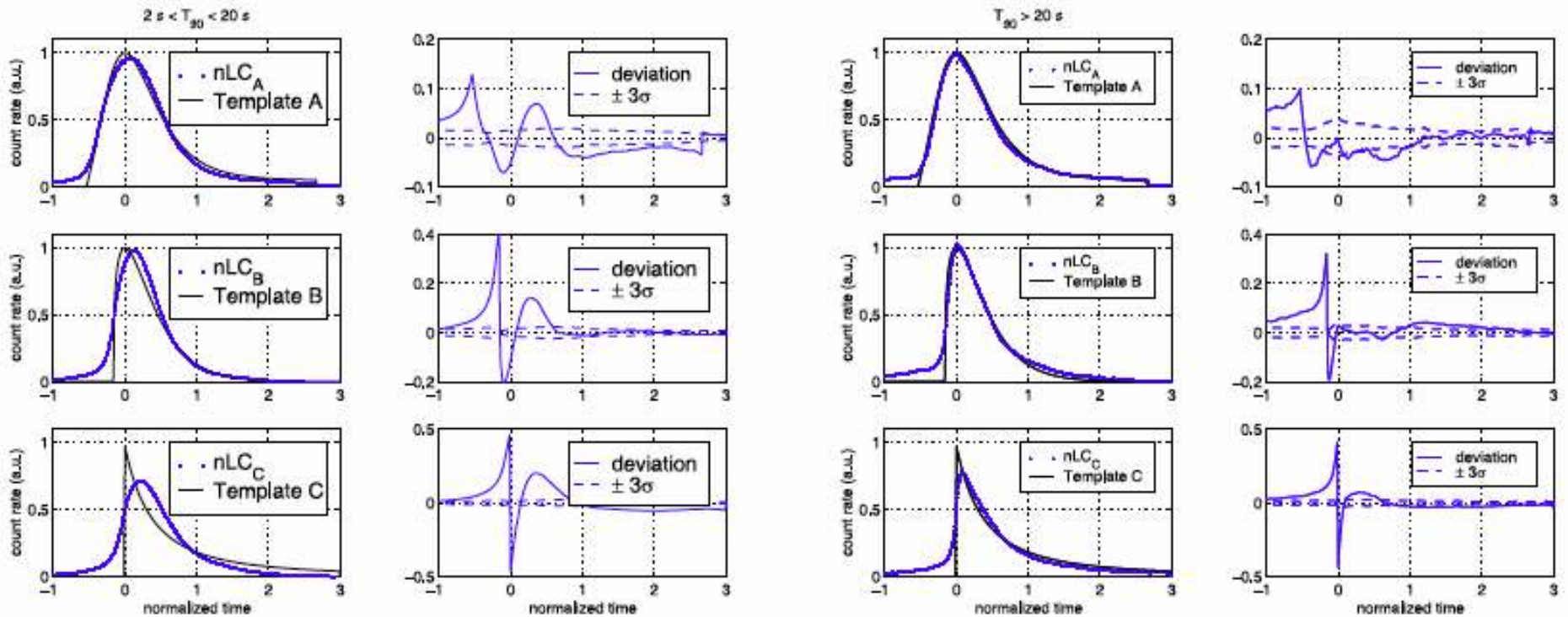


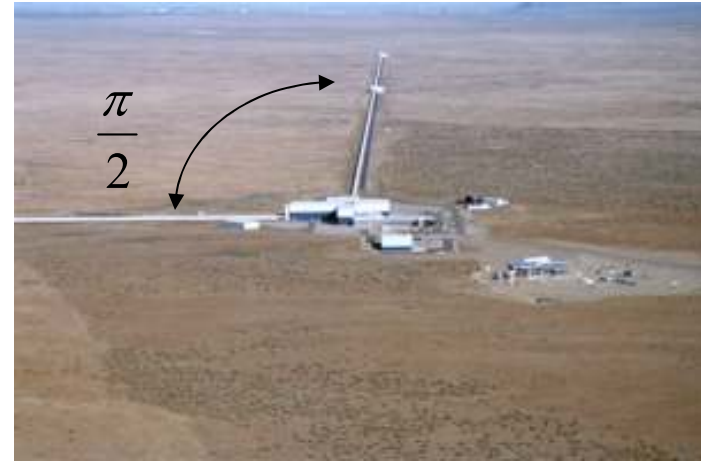
Fig. 6. Shown are the nLC (*circles*) generated by model templates A–C (*lines*) for the ensemble of 531 long duration bursts with $T_{90} < 20$ s (left) and the ensemble of 960 long bursts with $T_{90} > 20$ s (right). The standard deviation σ is calculated from the ensemble of individual nLCs. **Most favored: BH-spindown against ISCO**. **Least favored: NS spindown**

Outline

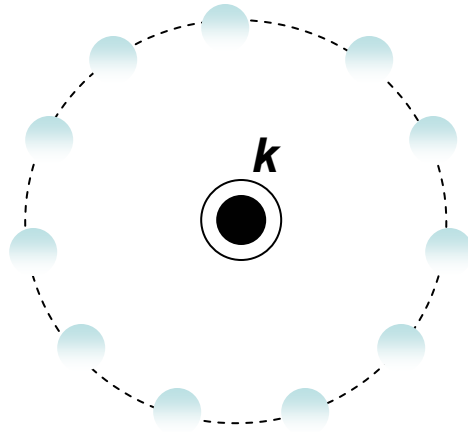
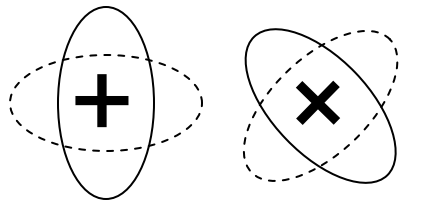
1. GRBs from rotating black holes
2. Probing BH-NS alternative for black hole spindown
- 3. Advanced gravitational wave detectors**
4. Outlook on broadband GW emission from CC-SNe

Gravitational-wave Detectors in US, EU and Japan

<http://www.ligo.caltech.edu>, <http://www.ego-gw.it>

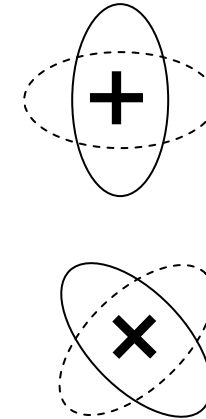


Ripples in spacetime

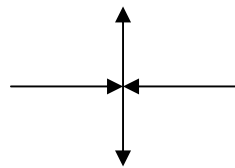


Ring of free particles in space

GW-modes



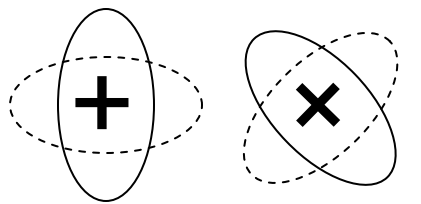
Transverse modes of radiation



Stretching and squeezing in orthogonal directions (area preserving)

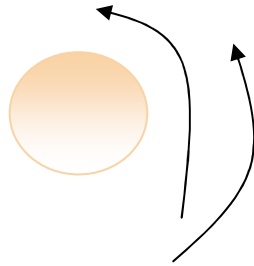
$$h = \frac{L_x - L_y}{L}$$

Dimensionless strain amplitude



Quadrupole GW emission from binaries

Kepler's law when separation $\gg R_g$



In geometrical units

$$R_g = \frac{GM}{c^2}, \quad s = ct$$

giving small angles

$$\alpha_i = \kappa M_i \quad (i=1,2), \quad \kappa = \frac{1}{a}$$

Matching dimensionless quantities in geometrical units

Luminosity $L_{GW} \sim \frac{\Delta E}{\Delta t}$

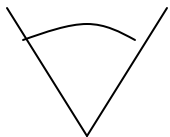
$$\Rightarrow L_{GW} \sim f(\alpha_1, \alpha_2) F \propto R_g^2 a^4 \omega^6$$

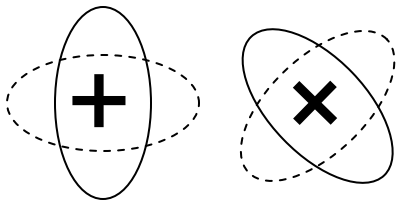
Force $F \sim \frac{M_1 M_2}{a^2} = \alpha_1 \alpha_2$

Quadrupole radiation in dimensionless strain amplitude

Strain $h \sim \frac{U}{D} \sim \frac{E_k}{D} \Rightarrow L_{GW} \sim 4\pi r^2 \dot{h}^2 \sim R_g^2 a^4 \omega^6$

D





Existing observations

Hulse-Taylor binary PSR 1913+16 (Nobel 1993)

$P \sim 7.75$ hr

$e \sim 0.6171338$

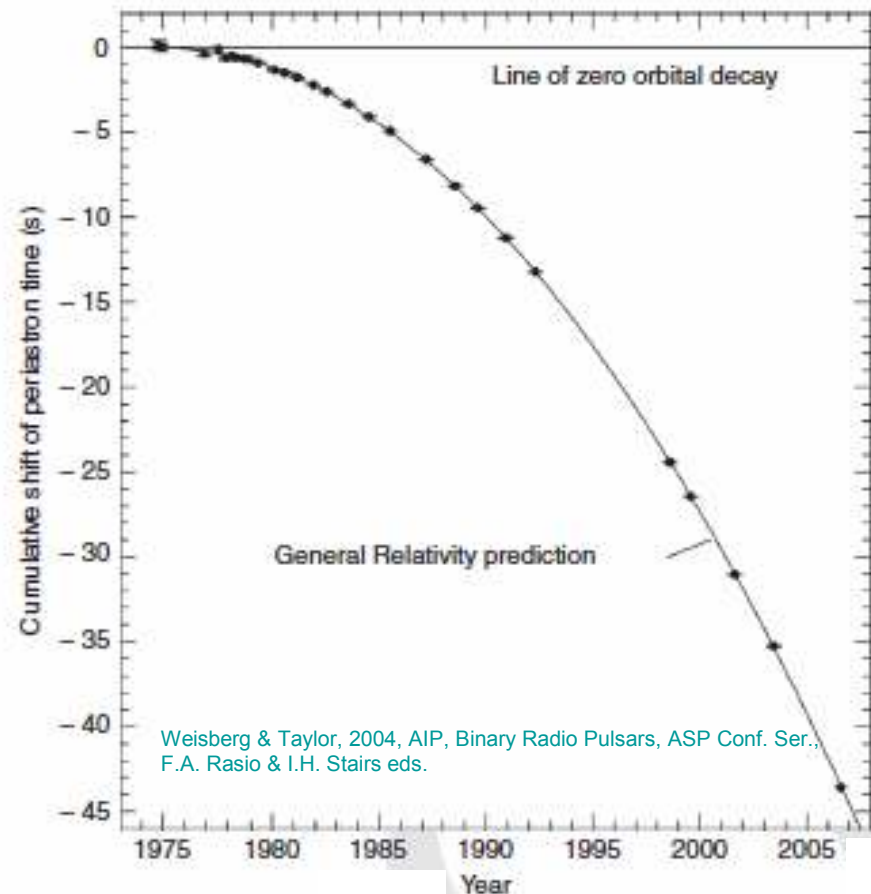
$L_{GW} \sim 7.35e24$ Watt (enhanced by e)

Time to coalescence ~ 300 Myr

$L_{GW} = 0.15\%$ of L_{sun} (3.8×10^{33} erg/s)

(includes enhancement by e)

Agreement with theory within 0.1%



(c)2014 van

GW emissions from a high density disk or torus

Quadrupole gravitational wave emission formula

$$L_{GW} = \frac{32}{5} (\mu_{chirp} \omega)^{\frac{10}{3}}, \quad \mu_{chirp} = \frac{M_1^{\frac{3}{5}} M_2^{\frac{3}{5}}}{(M_1 + M_2)^{\frac{1}{5}}}$$

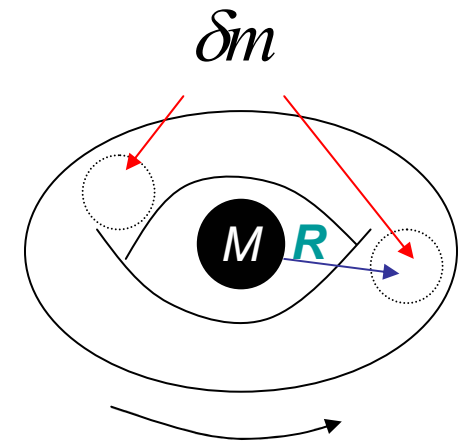
Conversion factor

$$\frac{c^5}{G} = 3.6 \times 10^{59} \text{ erg s}^{-1}$$

Apply to mass-inhomogeneities in orbital motion

$$L_{GW} \cong \frac{32}{5} \left(\frac{M}{R}\right)^5 \left(\frac{\delta m}{M}\right)^2$$

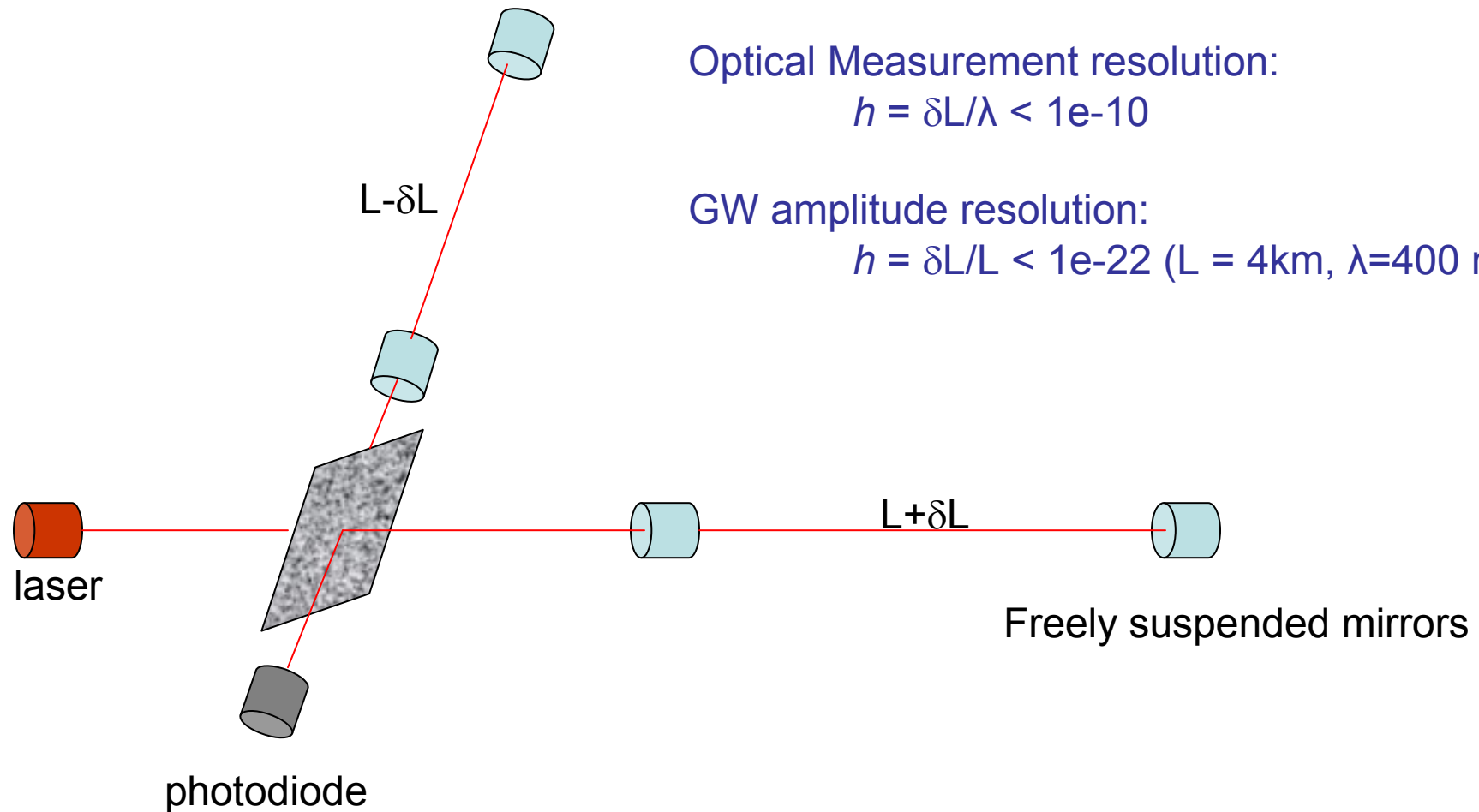
δm of about 10% of $M_D = 1\% M$, due to a wave excited by forced turbulence:



CC-SNe, LGRBs: $L_{GW} \cong 2 \times 10^{51} \text{ erg s}^{-1}$

SgrA*: $L_{GW} \cong 7 \times 10^{41} \text{ erg s}^{-1}$

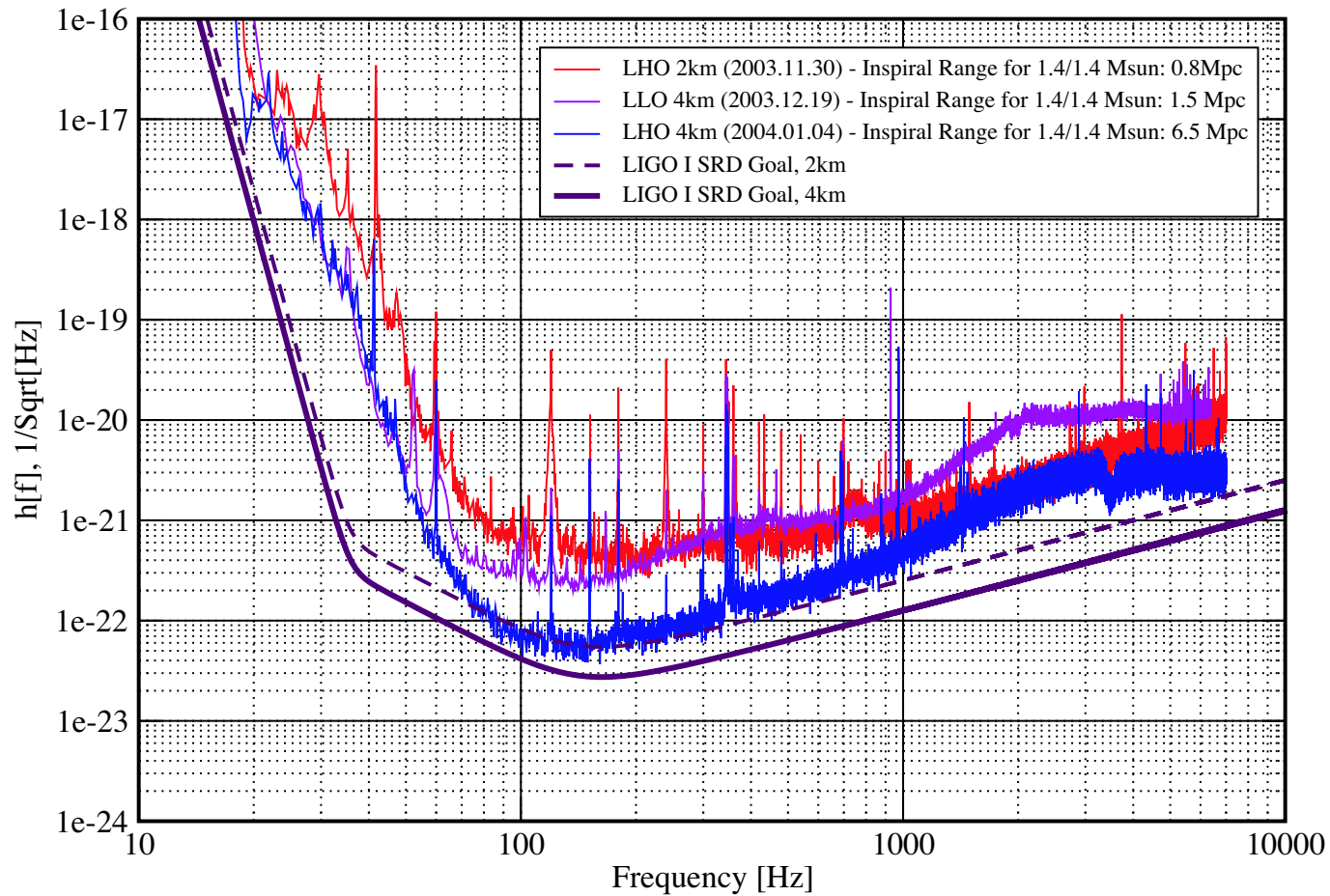
Laser Interferometry on GWs



Laser Interferometry: performance

Strain Sensivities for the LIGO Interferometers

Best S3 Performance LIGO-G040023-00-E



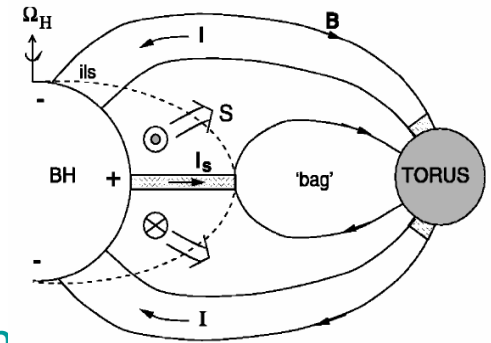
van Putten, 1999, Science, 284, 115, van Putten & Levinson, 2002, Science, 295, 1874
 van Putten, 2001, Phys. Rev. Lett., 84, 091101
 van Putten, 2002, ApJ, 575, L71
 van Putten, 2012, Prog. Theor. Phys., 127,331
 van Putten, 2008, ApJ, 684, L91

Long duration GW burst

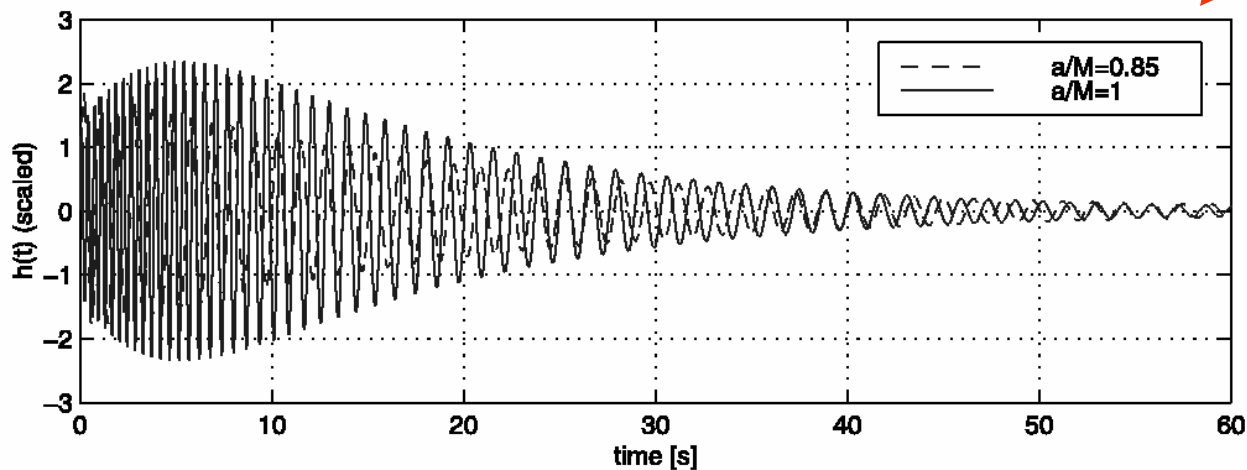
Flat IR MHD turbulent spectrum \rightarrow suspended accretion

Thermal and magnetic pressure induced instabilities \rightarrow LF GWs

Balance heating by dissipation in MHD turbulence with cooling in gravitational radiation



Anticipate gradual black hole spindown



Formation of mass-inhomogeneities

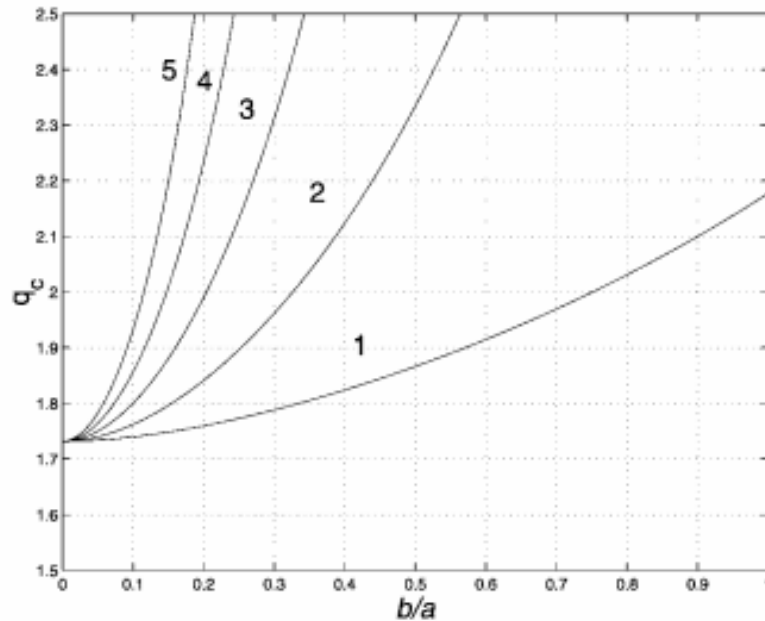
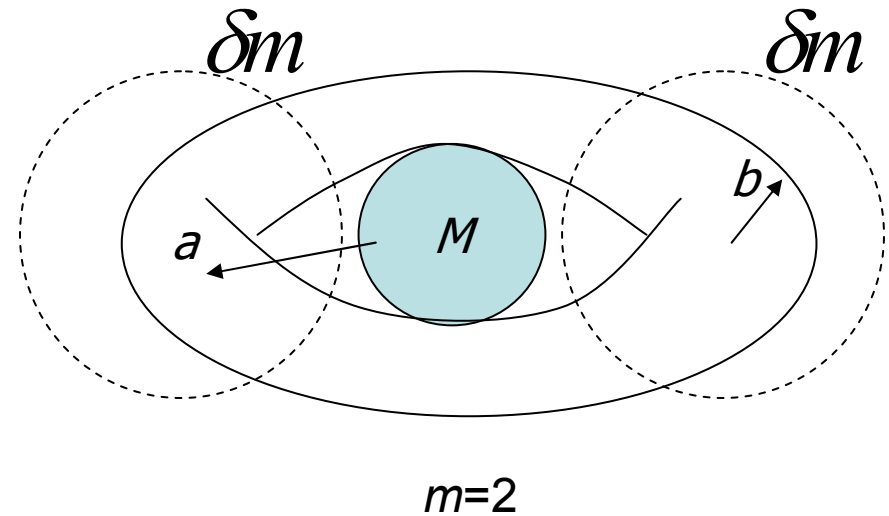


FIG. 2.—Diagram showing the neutral stability curves for buckling modes in a torus of incompressible fluid, as an extension of the Papaloizou-Pringle instability to large ratios of minor-to-major radius b/a . Curves of critical rotation index q_c are labeled with azimuthal quantum numbers $m = 1, 2, \dots$, where instability sets in above and stability sets in below. Of particular interest is the range $q \leq 2$, where the $m = 0$ mode is Rayleigh-stable. For $q = 2$, the torus is unstable for $b/a < 0.7385$ ($m = 1$), 0.3225 ($m = 2$) and, asymptotically, for $b/a \approx 0.56/m$ ($m \geq 3$).

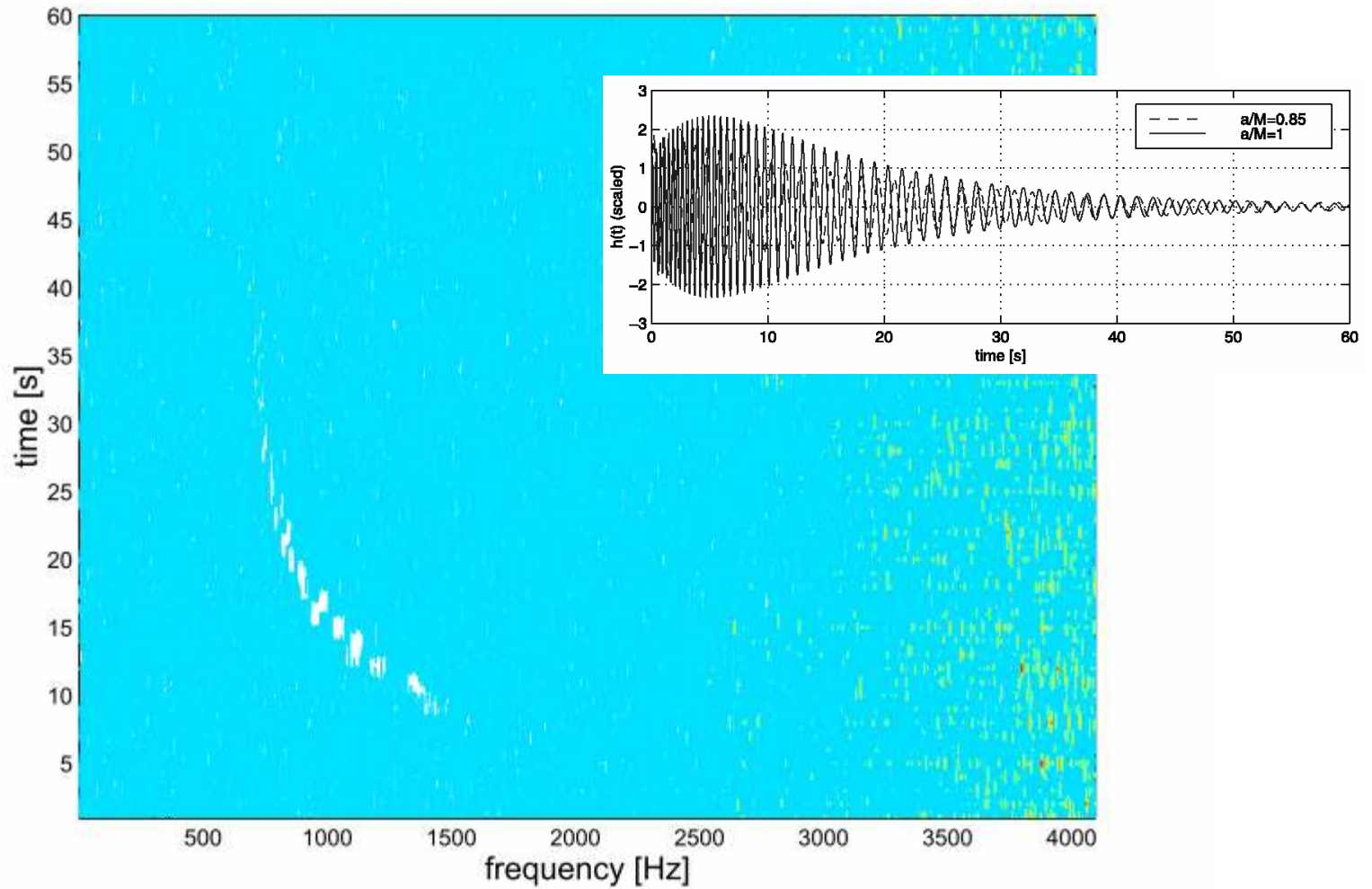


Wide tori are $m = 1, 2, \dots$ unstable

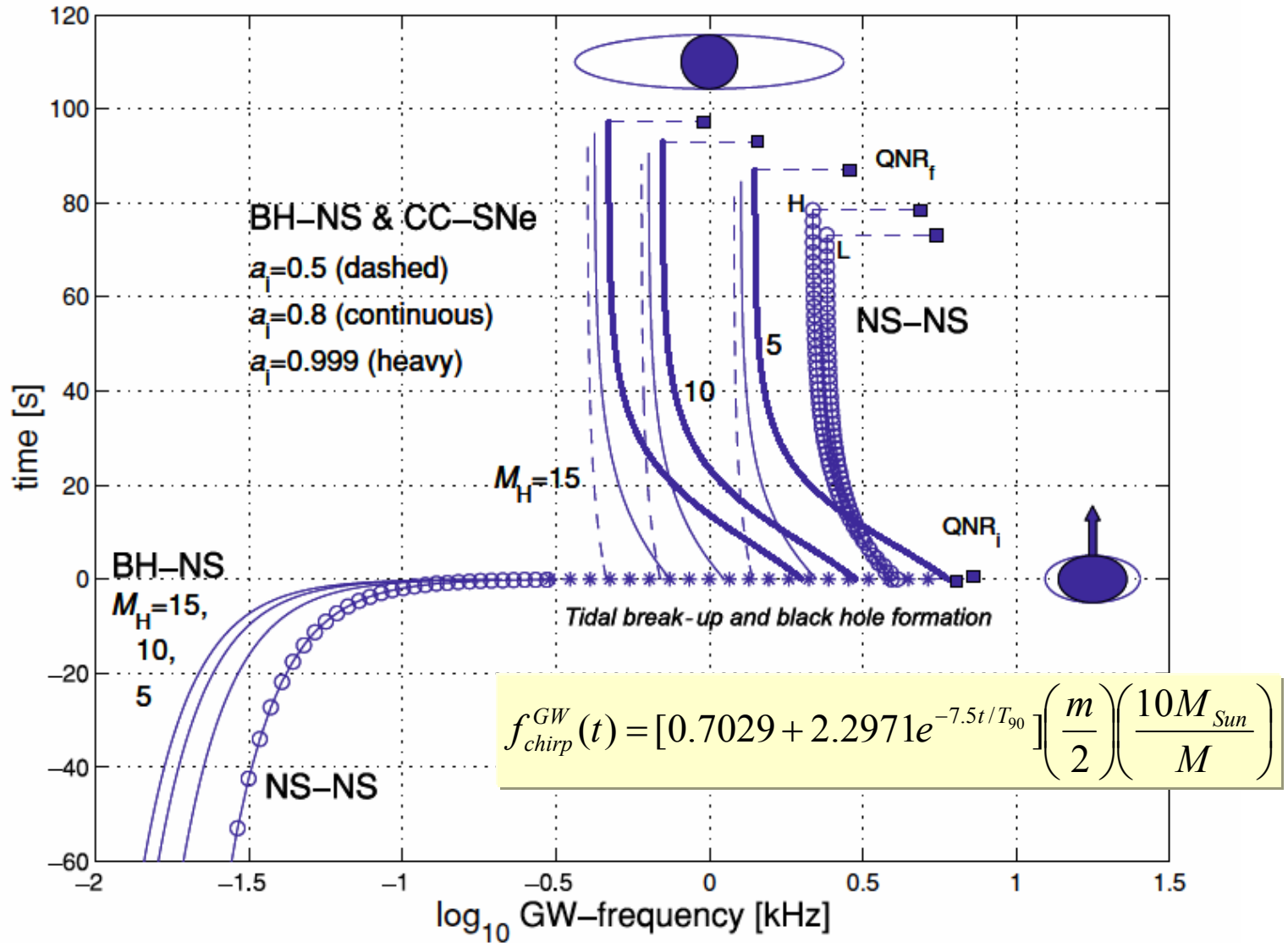
Lowest order modes are unstable first:

most of GW-emission from lowest order modes ~ LIGO-Virgo/KAGRA bandwidth

Negative chirp during black hole spindown

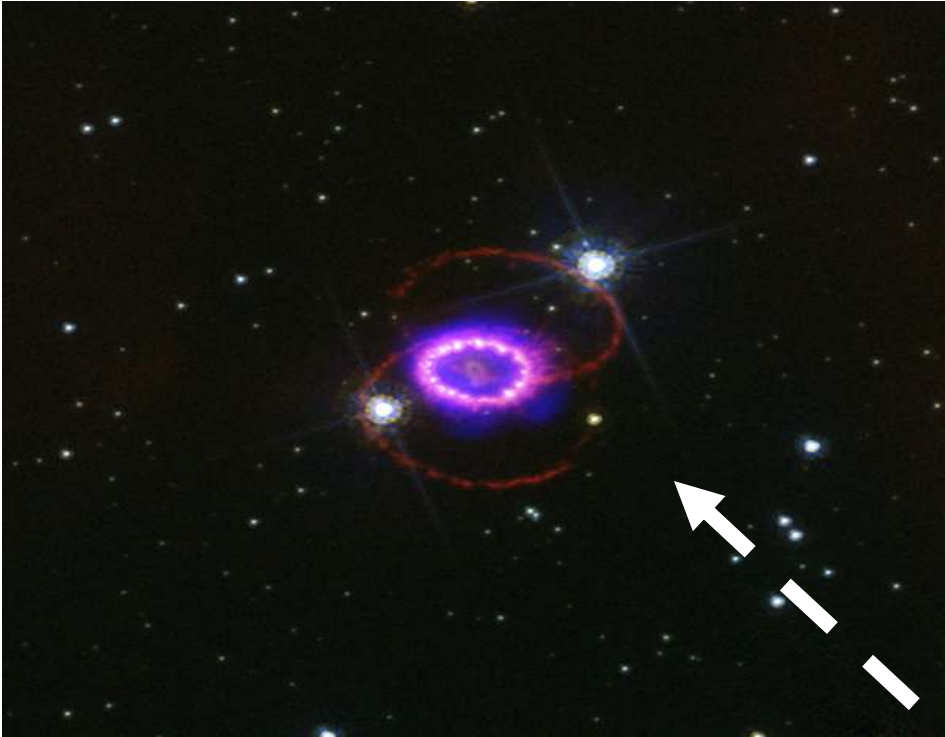


Chirp diagram

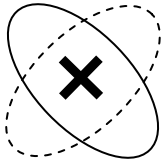
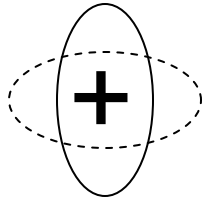


e.g. LIGO-VirgoScientific
Collaboration, 2013,
arXiv:1310.2314v1

Observational strategy



GW-modes



LIGO detector

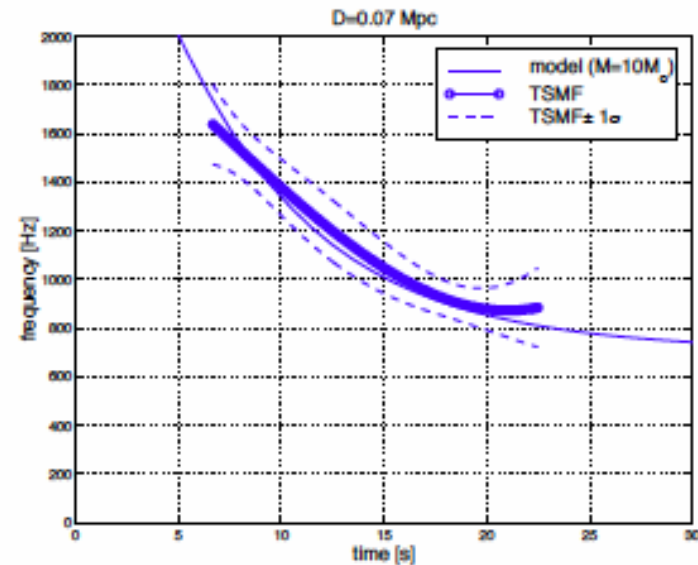
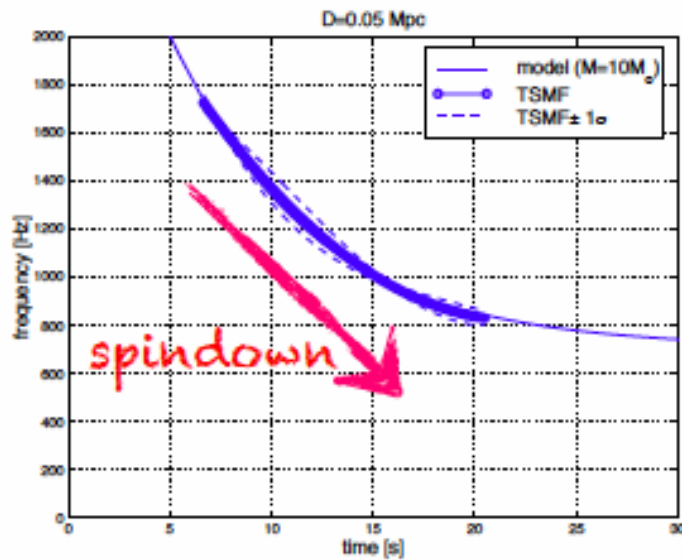




Original by P.C. Mondriaan (1872-1944)

GW detectors are near-sighted

Sensitivity distances by matched filtering

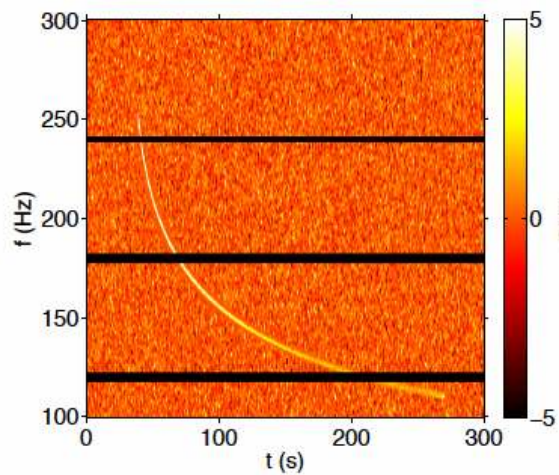


Advanced detectors (LIGO-Virgo, LCGT): $h \sim 2e-24 @ 1000\text{Hz}$

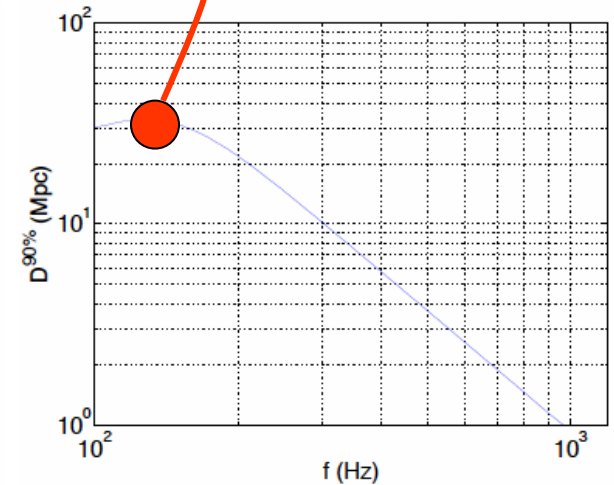
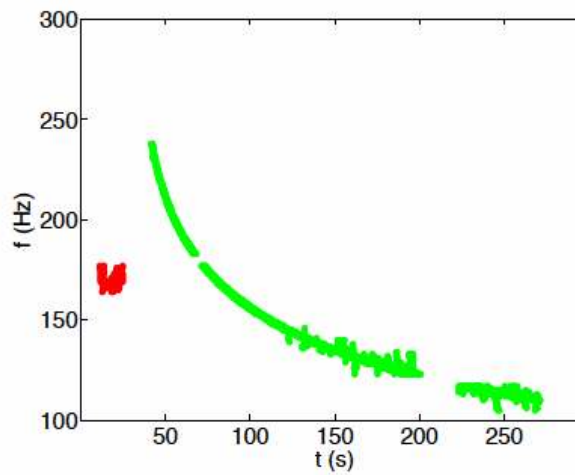
$$D \approx 35 \text{ Mpc}$$

Sensitivity distances by a clustering algorithm

GRB 070611 ($z=2.04$)



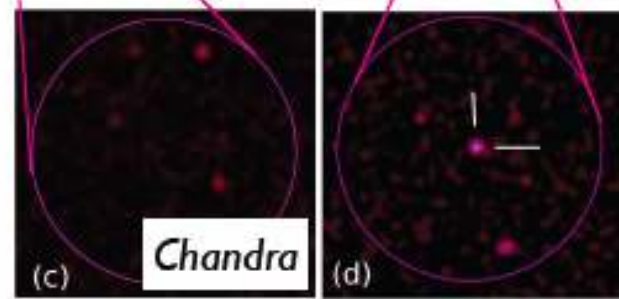
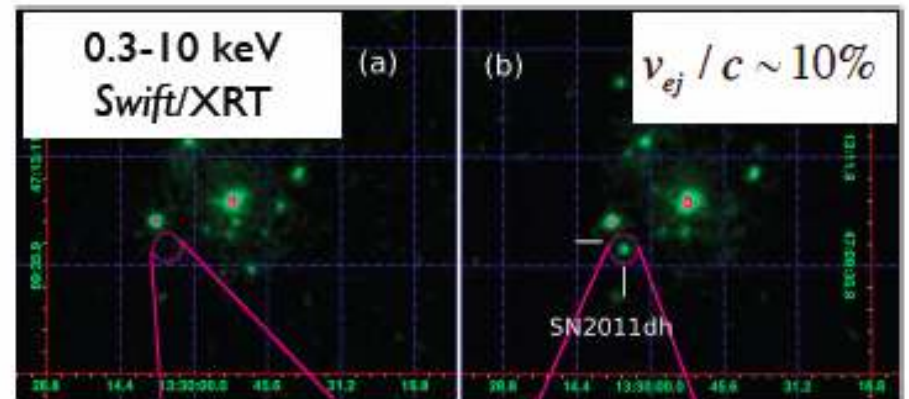
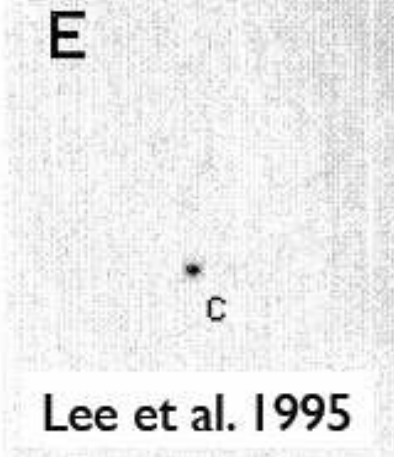
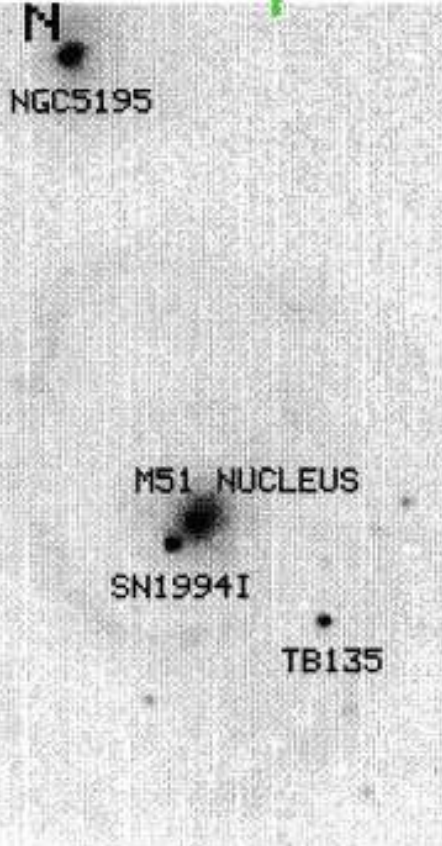
Negative chirp injected
into LIGO strain
amplitude detector
noise



$$E_{GW} = 0.1 M_{\odot} c^2$$

$$D_{sens} \sim 30 \text{ Mpc}$$

M51: farmland of CC-SNe at 8 Mpc



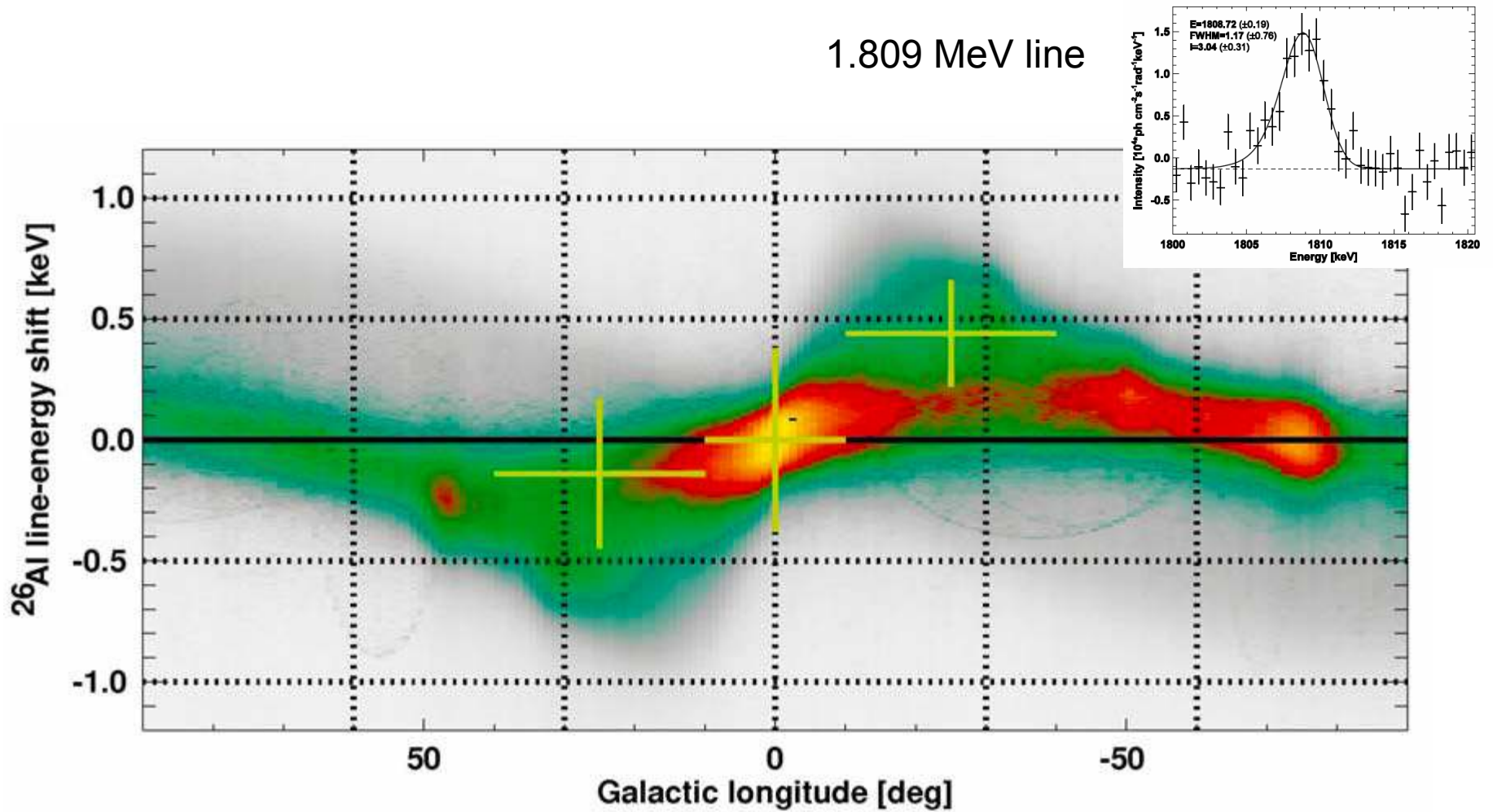
SN1994i: Type Ic, $M \sim 12-30$ solar
 SN2005cs: Type II, $M \sim 18.1$ solar
 SN2011dh: Type II-P, $M \sim 13$ solar

once every ~8.5 years?

Soderberg et al., 2011, arXiv:1107.1876

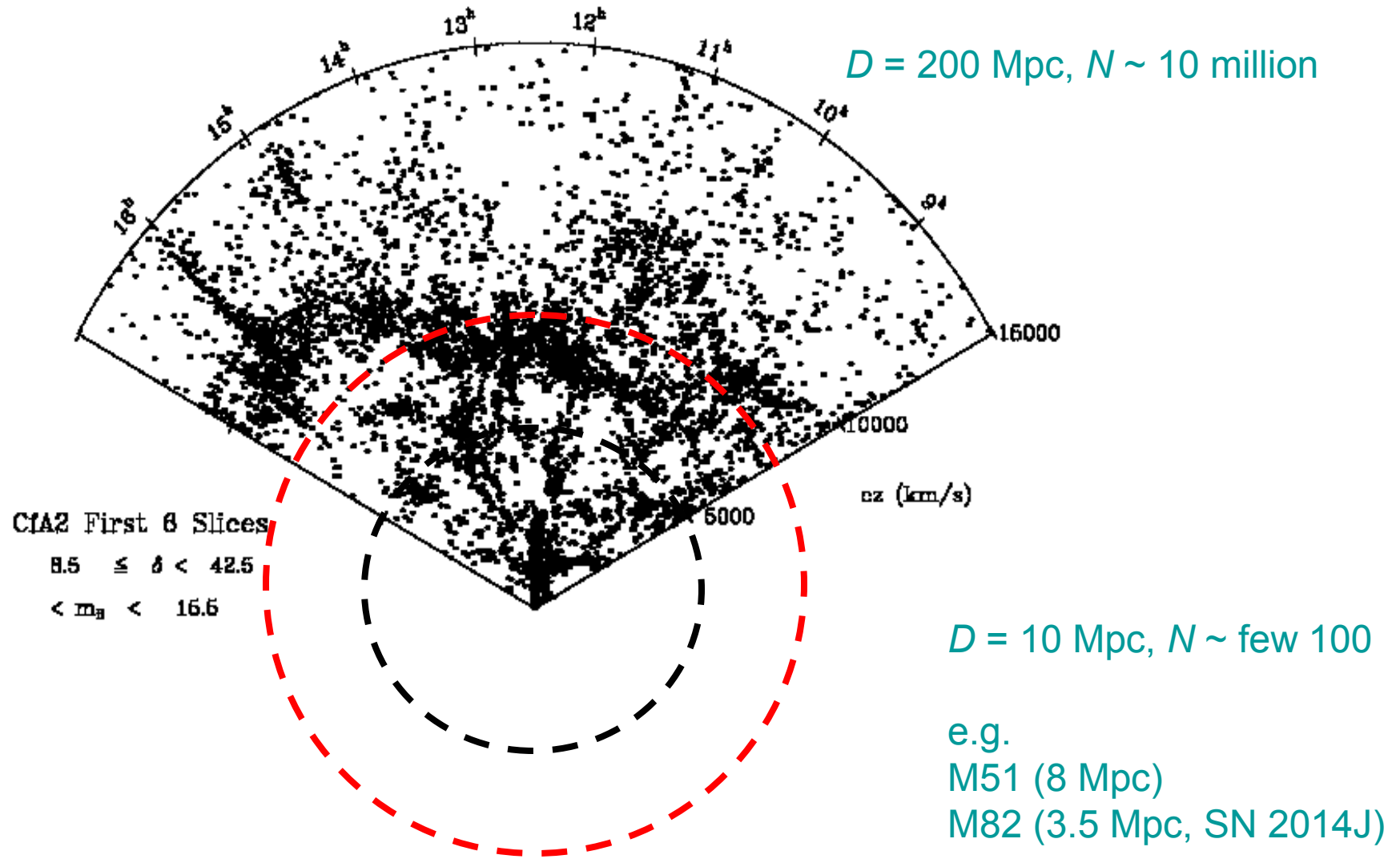
Local rates: Milky Way

1.809 MeV line

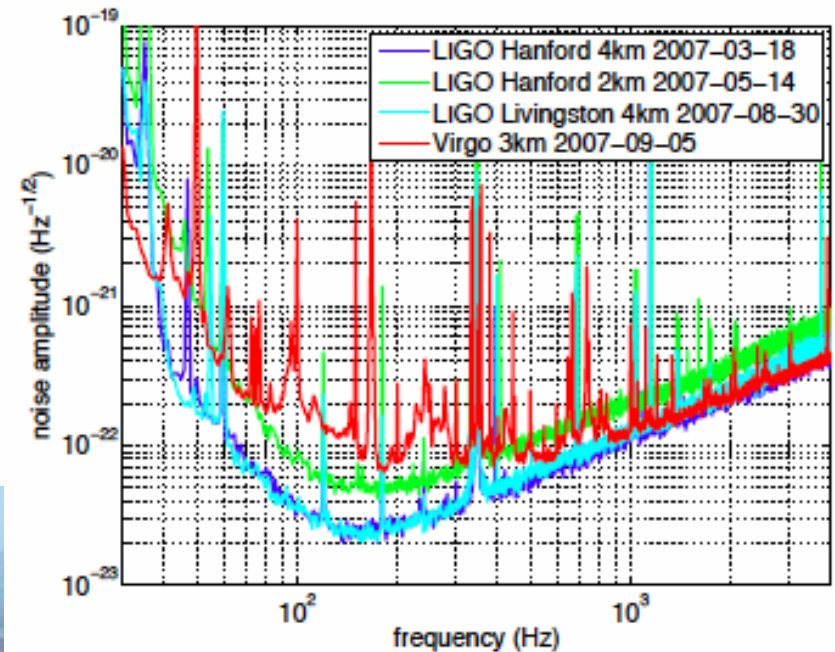
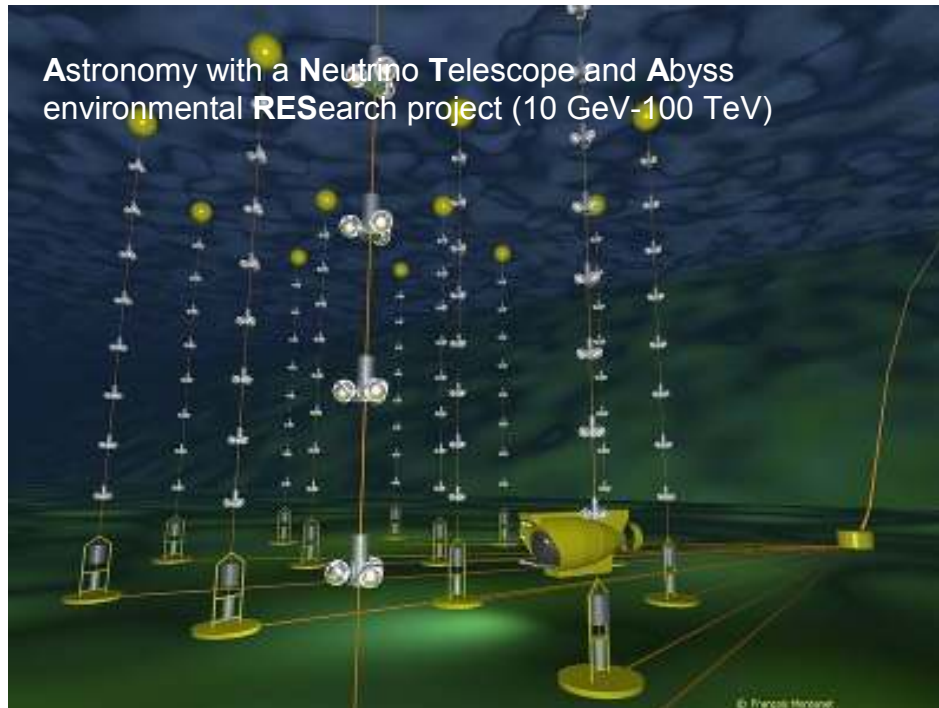


CC-SNe rate: 1.9(+/- 1.1) events / century

Desired: optical-radio survey < 35 Mpc



Search for coincident GW-HEN events



Start of multi-messenger astronomy
Need improvements by x10 for a realistic outlook for a detection

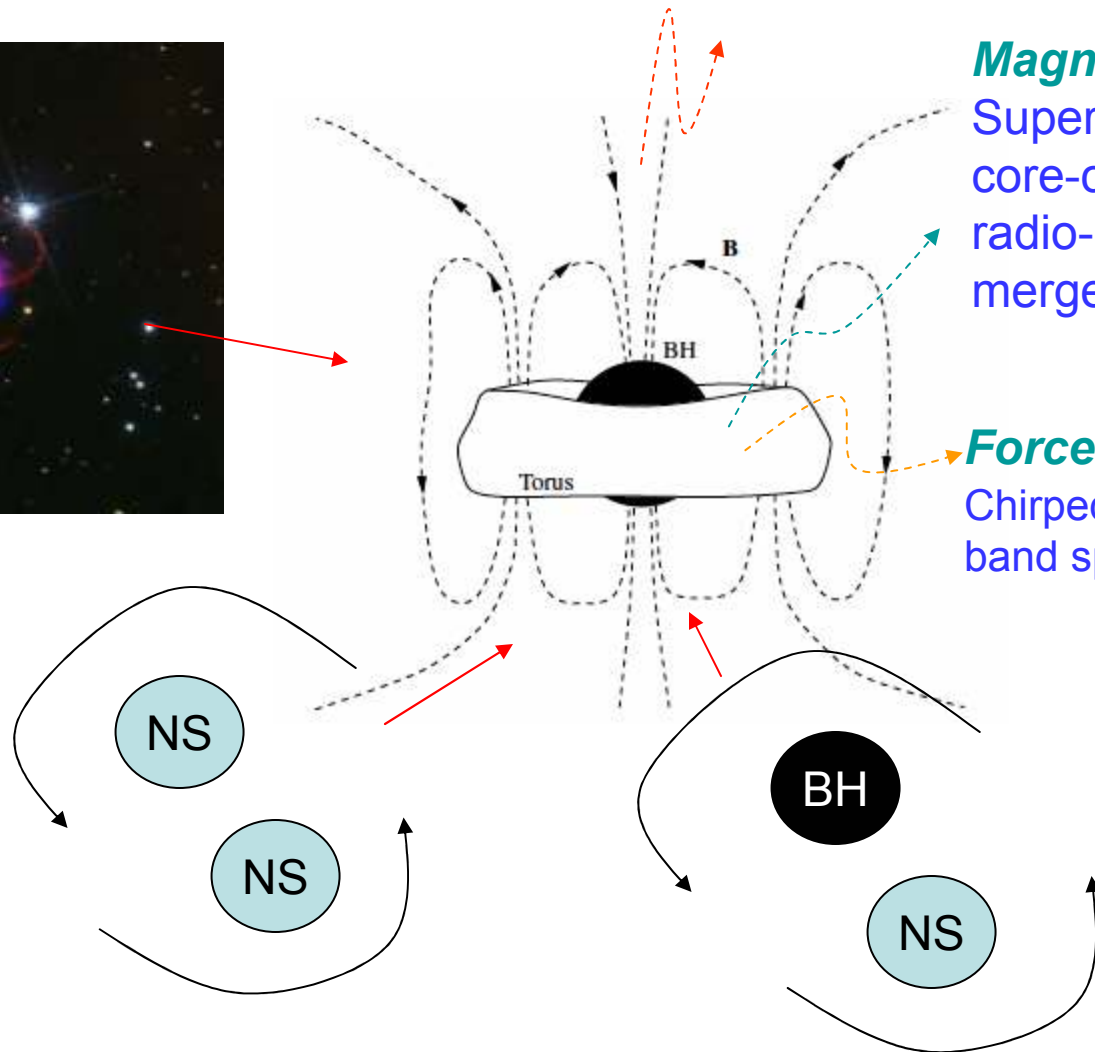


Multimessenger output from LGRBs

Baryon-poor jets:
LGRB, HEN

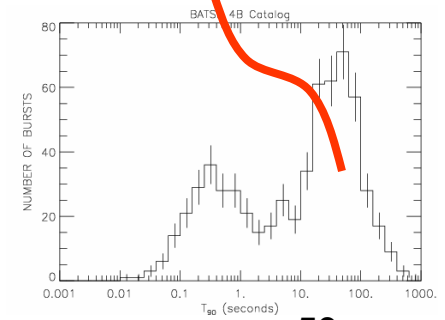
Magnetic winds:
Supernovae following core-collapse
radio-burst following mergers (LOFAR/SKA)

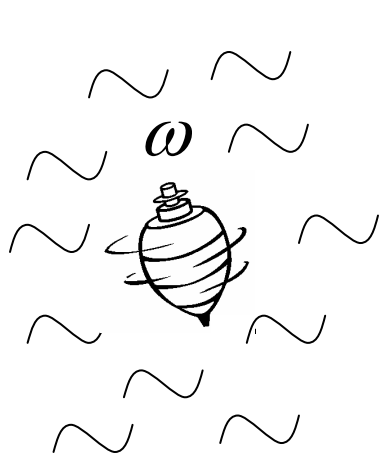
Forced MHD turbulence:
Chirped line- and broad band spectrum in GWs



$$E_{GW} \geq 0.1 M_s c^2$$

$$T \sim T_{90} [\text{GRB}]$$





Conclusions and outlook

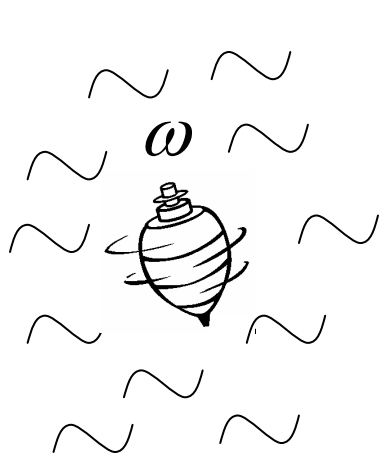
Unification in GRBs from rotating black holes:

-Short and long GRBs: $\begin{cases} \Omega_H < \Omega_{ISCO} : T_{90} \sim T_{hyper-accretion} \\ \Omega_H > \Omega_{ISCO} : T_{90} \sim T_{spin} \end{cases}$ Observed in nLC/BATSE

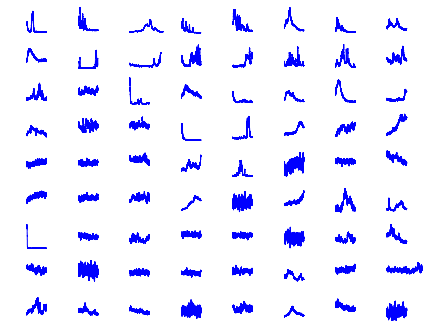
-Hyper-energetic GRB-SNe: $E > \eta^{-1} E_c$ [PNS]

-Orphan LGRBs from mergers involving rapidly rotating BHs

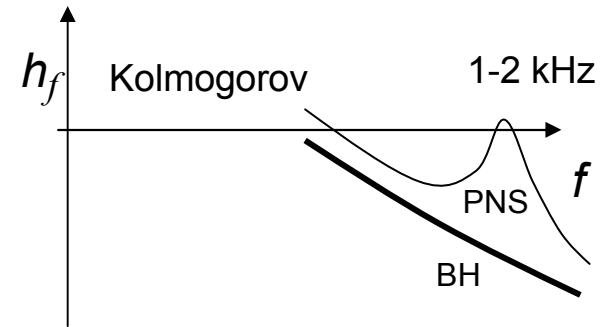
Conclusions and outlook



Search for rotation in HF windows (0-1000 Hz) to GRBs and CC-SNe for direct detection of a turbulent accretion disk:



Searches in 2 kHz GRB light curves (BeppoSax, Swift, future missions) for HF modulations



Searches in nearby CC-SNe for GWs (LIGO-Virgo/KAGRA): chirped line emission and broad band emission from multiple mass-moments

